Kaunas University of Technology

Faculty of Electrical and Electronics Engineering

Investigation of Analog Phase Shifters for 5G Applications

Master's Final Degree Project

Sithara Moloth Valappil

Project author

Dr. Merfeldas Audrius

Supervisor

Kaunas, 2023

Kaunas University of Technology
Faculty of Electrical and Electronics Engineering

Investigation of Analog Phase Shifters for 5G Applications

Master's Final Degree Project

Electronic Engineering (6211EX012)

Sithara Moloth Valappil
Project author

Dr. Merfeldas Audrius
Supervisor

Prof. Darius Gailius
Reviewer

Kaunas, 2023

Kaunas University of Technology
Faculty of Electrical and Electronics Engineering
Sithara Moloth Valappil

Investigation of Analog Phase Shifters for 5G Applications

Declaration of Academic Integrity

I confirm the following:

1. I have prepared the final degree project independently and honestly without any violations of the copyrights or other rights of others, following the provisions of the Law on Copyrights and Related Rights of the Republic of Lithuania, the Regulations on the Management and Transfer of Intellectual Property of Kaunas University of Technology (hereinafter – University) and the ethical requirements stipulated by the Code of Academic Ethics of the University;

2. All the data and research results provided in the final degree project are correct and obtained legally; none of the parts of this project is plagiarised from any printed or electronic sources; all the quotations and references provided in the text of the final degree project are indicated in the list of references;

3. I have not paid anyone any monetary funds for the final degree project or the parts thereof unless required by the law;

4. I understand that in the case of any discovery of the fact of dishonesty or violation of any rights of others, the academic penalties will be imposed on me under the procedure applied at the University; I will be expelled from the University and my final degree project can be submitted to the Office of the Ombudsperson for Academic Ethics and Procedures in the examination of a possible violation of academic ethics.

Sithara Moloth Valappil

Confirmed electronically

Moloth Valappil Sithara. Investigation of Analog Phase Shifters for 5G Applications / Master's Final Degree Project/ Dr. Merfeldas Audrius; Faculty of Electrical and Electronics Engineering, Kaunas University of Technology.

Study field and area (study field group): Electronics Engineering, Engineering Sciences

Keywords: Reflection Type Phase Shifter, S Parameters, Insertion loss, Reflection loss

Kaunas, 2023. 57 p.

Summary

This work investigates Reflection Type Phase Shifters and compares and optimises three different phase shifter models. The operating frequency is 3.5 GHz and the measurements are done at 3.3 GHz, 3.5 GHz and 3.8 GHz frequencies. Reflection coefficients, insertion losses, phase shift and VSWR are measured. A reflection coefficient which is more negative than -15 dB, insertion loss which is more than -2 dB and a minimum VSWR value are expected. The behaviour of the different models of phase shifters is analysed based on these requirements. Other than these parameters, the bandwidth performance of each model is also compared. Phase shifts against variable load graphs are plotted using MATLAB for each model.

Moloth Valappil, Sithara. Analoginių fazių keitiklių, skirtų 5G programoms, tyrimas . Magistro baigiamasis projektas/ Dr. Merfeldas Audrius; Kauno technologijos universitetas, Elektros ir elektronikos fakultetas.

Studijų kryptis ir sritis (studijų krypčių grupė): Elektronikos inžinerija, inžinerijos mokslai

Reikšminiai žodžiai: atspindžio tipo fazės keitiklius, S parametrai, įterpimo nuostoliai, atspindžio koeficientas,

Kaunas, 2023. 57 p.

Santrauka

Šiame darbe tiriami atspindžio tipo radijo dažnių signalų fazės keitiklius. Darbe lyginami bei optimizuojami trijų skirtingų fazių keitiklių modeliai. Centrinis dažnis yra 3.5 GHz, tačiau matavimai yra atlikti pasirinkus kampinius 3.3 GHz, 3.5 GHz ir 3.8 GHz dažnius. Atspindžio koeficientas, įvesties nuostoliai, fazės postūmis ir VSWR yra analizuoti modeliuojant CST Studio Suite aplinkoje. Atspindžio koeficientas mažesnis nei -15 dB, įterpimo nuostoliai, mažesni nei -2 dB, bei minimali VSWR reikšmė yra pagrindiniai skirtingų tipų vertinimo rezultatai. Be šių kriterijų taip pat tarpusavyje buvo palygintas ir kiekvieno modelio darbinis dažnių ruožas. Fazės poslinkio priklausomybės nuo kintamųjų pateiktos grafikuose, nubraižytuose panaudojus MATLAB programinį paketą.

Table of contents

List of Figures

List of Tables

List of abbreviations and terms

Abbreviations:

μm – micrometre

5G – Fifth Generation

BLC - Branchline Coupler

CST – Computer Simulation Technology

dB – Decibel

eMBB - Enhanced Mobile Broadband

FR-4 – Flame Retarded

Gbps – Giga bites per second

GHz – Giga Herts

IoT – Internet of Things

ITS - Intelligent Transportation System

Massive MIMO – Massive Multiple Input Multiple Output

MHz – Mega Herts

mm – milli meter

mMTC - Massive Machine Type Communications

mmWave – Millimeter Wave

ms – milli second

nH – nano Henry

PCB – Printed Circuit Board

pF – Pico Farad

RF – Radio Frequency

RTPS - Reflection Type Phase Shifter

SIW - Substrate Integrated Waveguide

URLLC - Ultra Reliable Low Latency Communications

VSWR – Voltage Standing Wave Ratio

Introduction

5G has brought notable differences to our day-to-day life even when the current implementation has not reached the peak of the technology's capacity. High-speed internet possibilities are connecting us more closely than ever. The quality of the calls has improved and faster connectivity is achieved by 5G.

Phase shifters are an important part of 5G technology. 5G is exploiting the higher frequencies that have not been used before and have shorter wavelengths and are prone to more attenuation. Hence the antenna beam should be focussed and thus the energy can be saved as well. The technique, Massive MIMO which improves the spectral efficiency is the backbone of 5G consisting of thousands of antenna elements in the base station antenna. The beam steering to the desired direction in a system with antenna arrays is established by using phase shifters. Before each element of the antenna array, a phase control or phase shifter is placed. It makes it possible to steer the beam without any moving parts.

Phase shifter technologies vary from switching techniques where we add additional lines to delay signals to change the phase to modern technologies of digitally controlled phase shifters. Analog phase shifters play a very important role because we can control the phase with the highest precision with no steps in phase control as in digital phase shifters. Reflection type phase shifters are an important type with a 3 dB hybrid couplers part with reflective loads at through port and coupled port introduces a phase shift. They provide continuous phase shifts and good return loss.

Aim: Analysis and investigation of analog reflection-type phase shifters at 3.5 GHz frequency for 5G applications.

Objectives:

1. Study of different designs of reflection-type phase shifters.
2. Modelling of reflection-type phase shifters with a single-section branch-line coupler, two sections branch-line coupler and with a high impedance line in front of the load, consisting of tunable loads.
3. Evaluation and comparison of different designs based on their phase shift, bandwidth, and losses.

1. Literature Analysis

1.1. Fifth-generation broadband cellular network

In Telecommunications, the evolution (Fig.1) is based on the increased number of services and the speed and stability of connectivity [1]. Compared to the legacy 4G network, the latency is reduced from 10 ms to 1 ms, maximum data rates are increased from 1 Gbps to 20 Gbps, available spectrum is increased from 3 GHz to 30 GHz and the number of devices connected is increased from 100 thousand to 1 million per square kilometre area [20]. Considering all these, 5G provides better quality of service and supports IOT applications.

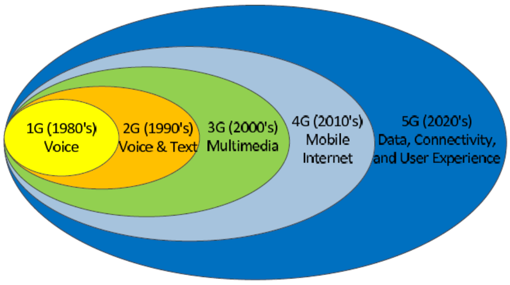

Fig. 1. Cellular Communication Evolution [1]

The fifth generation of broadband cellular network or 5G Technology has the following important areas of application.

- Enhanced Mobile Broadband (eMBB) – Improved throughput, connection establishment and capacity
- Ultra Reliable Low Latency Communications (URLLC) [42] – Stable connection with reduced lag
- Massive Machine Type Communications (mMTC) – Connection of devices in huge numbers.

The advantages can also be referred to as challenges (Fig. 2) due to complex architectural requirements [2,3].

Fig. 2. Challenges of 5G systems [2,3]

1.2. 5G Frequencies

5G spectrum has divided into two namely, sub-6 GHz and millimetre wave(mmWave) frequencies. These are also known as FR1 (FR stands for Frequency Range) and FR2 respectively.
FR: 450 MHz - 6 GHz
FR2: 24.25 GHz - 52.6 GHz (microwave bands (3 – 30 GHz) and Milli meter [4] (mmWave, 30 – 300 GHz)
Fig. 1 gives a clear picture of the nG spectrum [1].

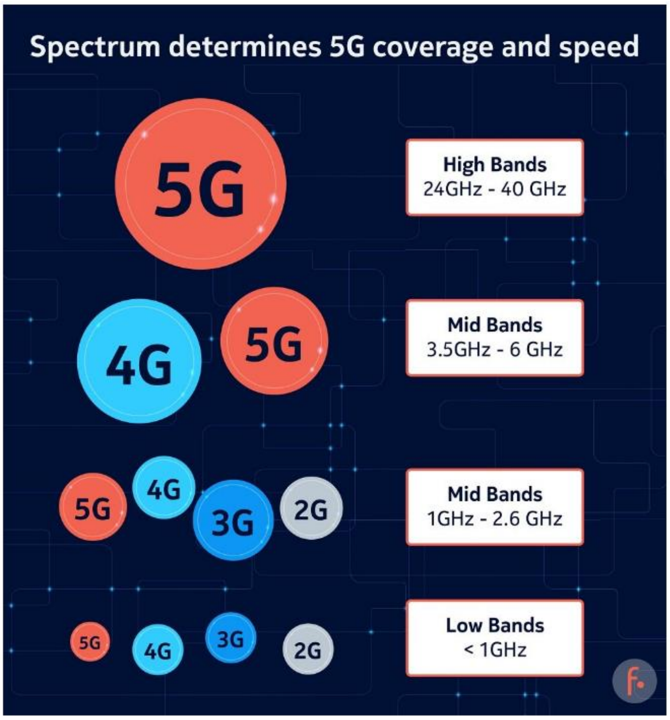

Fig. 3. nG Frequency spectrum [1]

Implementation of 5G makes use of spectrum sharing with LTE frequencies by Time Division Duplexing (TDD) or Frequency Division Duplexing (FDD) [21]. Frequency use depends on the population of a certain area, lower frequencies are enough in less densely populated regions because the signal will not get attenuated while travelling longer distances.

This work chooses the frequency of operation as 3.5 GHz. This frequency is the most tested 5G frequency and belongs to the C band of the 5G frequency [2]. Evaluations are done at three different frequencies. 3.3 GHz, 3.5 GHz and 3.8 GHz since the band ranges from 3.3 GHz to 3.8 GHz.

1.3. Phase Shifters

1.3.1. Importance of Phase Shifters

5G technology deals with higher frequencies compared to legacy technologies. Hence the wavelengths will be smaller so the length or size of the antenna. This results in the signal range being limited or the possibility of being affected by the obstacles. This leads to the need for a greater number of repeaters in between transmitter and receiver to enhance the signal and also phase shifters. Steering the signal in the desired direction with fewer obstacles is possible at the transmitter and receiver sides to adjust the direction in a way, it transmits a strong signal and captures the maximum signal coming. In 5G, not just one antenna is being used but antenna arrays (Fig. 4).

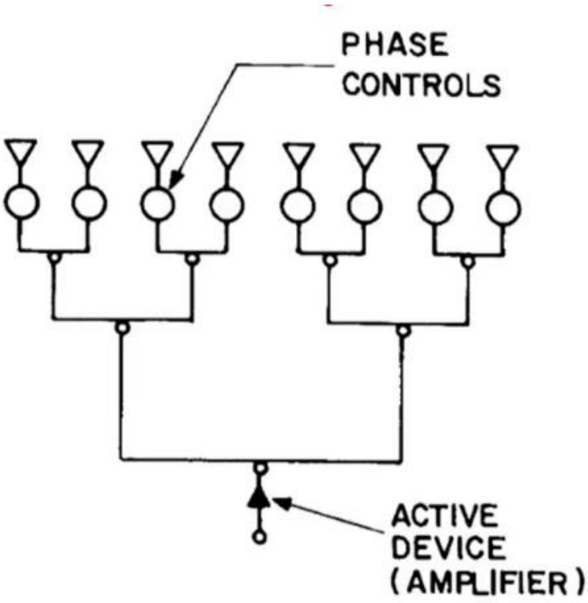

Fig. 4. Phased Array Antenna [4]

For better transmission and reception as mentioned, the Beamforming technique [3] is used, which provides directivity to the transceiving and is achieved by giving phase shift to the signals from different antenna elements of the phased array antenna, (Fig. 5).

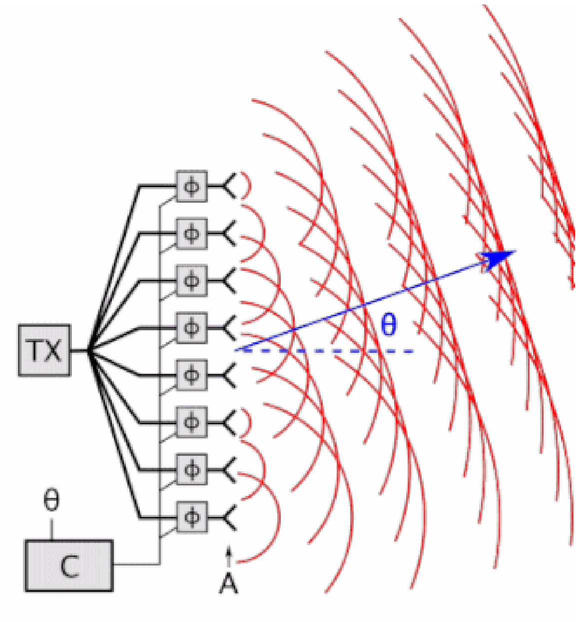

Fig. 5. Beamforming [5]

1.3.2. Comparison of Phase Shifters - Analog and Digital

Phase shift is introduced by providing a time delay to the signals. The easiest way to achieve this is by varying the length of the transmission line. What controls this process is what classifies phase shifters into analog or digital. The basic difference is that the phase shift is continuously variable in analog, which is typically controlled by a voltage. Varactor diodes, which vary the capacitance with reverse bias voltage are used to electrically control the analog phase shifters. They can also be mechanically controlled by controlling the length of the transmission line. Such lines are called Trombone lines.

Digitally controlled phase shifters are more in use since the effect of noise on the voltage control part is less. Digital phase shifters offer a discrete set of phase states which are controlled by two-state "phase bits." The 360 degrees are broken into smaller binary steps could be. The highest order bit is 180 degrees, followed by 90 degrees, 45 degrees, and so on. The least significant bit (LSB) of a phase shifter with three bits is 45 degrees, whereas a phase shifter with six bits has a 5.6-degree LSB. The advantages and disadvantages of Analog and Digital phase shifters [7] are summarised in Table 1.

Table 1. Analog and Digital Phase Shifter – Comparison [7]

	Analog	Digital
Advantages	• Precise phase shift values • Lower loss • Lower cost	• Noise immunity on the control line part • Less affected by impedance matching issues such as phase-pulling • Assembling is simple • Can manage large power • Linear phase
Disadvantages	• Prone to more noise	• Expensive in the case of antenna arrays having a huge number of antenna elements

The minimum phase shift obtained in the digital case is about 1 degree. 1 degree is unsuitable for high precision and distant objects like satellite communications. It is better to go for analog phase shifters to have a more precise phase shift. Also, while considering the 5G applications, the number of antenna elements in the antenna array is hundreds or thousands (Massive MIMO [5, 6]) and it will be expensive to use digital phase shifters.

Analog phase shifters are being used in electronic systems operating in the microwave and millimetre wave frequencies. Even though there is no digital control possible, and hence stability regarding the electrical performances analog phase shifters show low losses and the phase adjustment is more precise. Analog phase shifters can give a full cycle (360 degrees) phase shift, hence the integration to the radiating part of the phased array antenna is direct.

The requirements of phase shifters are:

- Phase shift and frequency
- Matching – Impedance matching
- Ripple – Variation in transmission losses
- Insertion loss
- Average losses

1.3.3. Types of Phase Shifters

Phase shifters are categorised mainly into four as follows [7].

1) Switched Line: Switch between transmission lines of different lengths to introduce phase shift
2) Reflection type: Relative phase shift between input and output is obtained by varying the reflection load.
3) Loaded line: When switched to the circuit, phase change is obtained according to load.
4) Low pass/High pass realisation: Near constant phase shift over an octave, one arm provides low pass and the other high pass characteristics

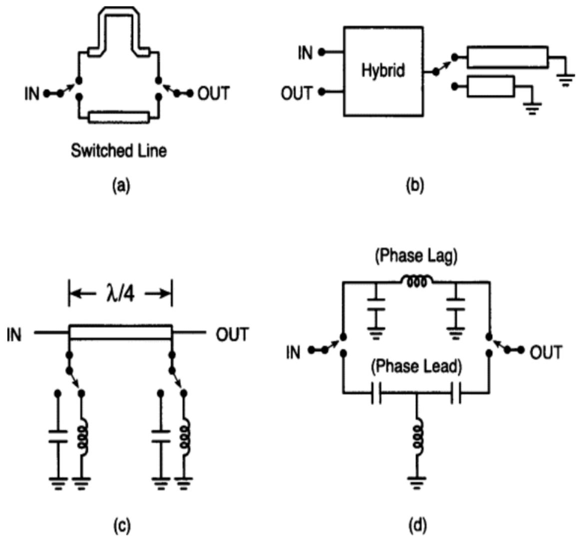

Fig. 6. Phase shifter types (a) switched line (b) reflection type (c) loaded line phase shifter (d) low-pass or high-pass type [7]

These types of phase shifters are different from each other considering the realization and the parameters such as frequency range, reflection coefficient and insertion loss.

1.3.4. Reflection Type Phase Shifter

The phase shift between input and output for reflection phase shifters is obtained by varying the reflection load. This method can give a wider sweep considering the use of a varactor diode/ varicap as the load. The voltage-controlled load can be designed in different ways as also the coupler part of the design.

1.3.5. Other Application Areas of Phase Shifters

Other than the Phased array antenna application of phase shifters in 5G, phase shifters are used in [14]:

- RADAR systems phased arrays
- Frequency translators
- Amplitude and phase modulation
- In SSPA (Solid State Power Amplifiers)
- Noise measurement on residual phase
- Phase correction of the signal in long-distance optical fibre communication.

Phased arrays are used in Starlink internet constellations by SpaceX [15,16]. The satellites are Low Earth Orbit satellites that require quick and high directivity with electronic tunability. Hence phase shifter applications can be found there as well.

1.4. Transmission Lines

A transmission line is a link that sends energy from one location to another. The study of transmission line theory aids in the efficient use of power and equipment. Different types of microwave transmission lines are [6]:

1) **Co-Axial:** High-frequency applications
2) **Strip Line:** Suitable for frequency 100 MHz to 100 GHz.
3) **Microstrip line:** Active and passive elements can be mounted and after the fabrication, minor adjustments are possible to the circuit.

Fig. 7 shows these three main transmission line types.

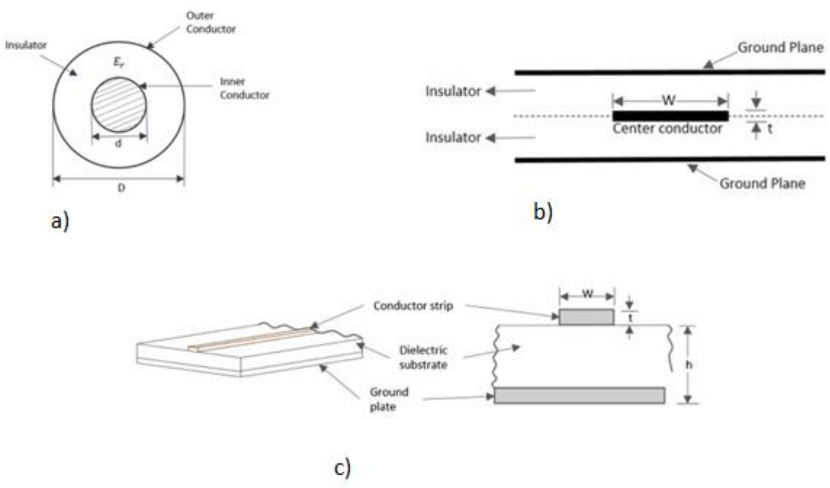

Fig. 7. (a) Co-Axial line, cross-sectional view (b) Strip lines (c) Microstrip line [6]

Some other types of transmission lines are shown in Fig. 8.

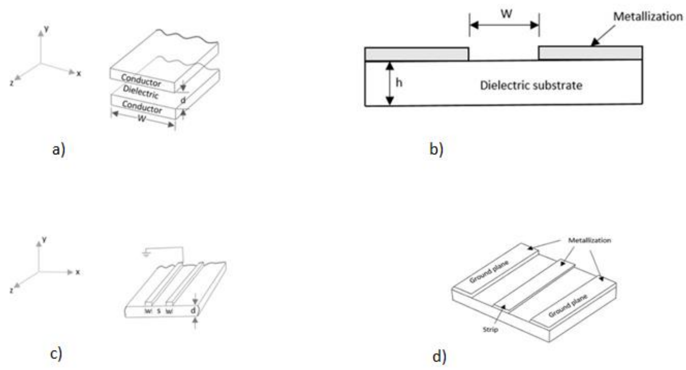

Fig. 8. Parallel Strip lines, (b)Slot line, (c) Coplanar strip line, (d) Co planar waveguide [6]

Different types of transmission lines are chosen for different applications. The microstrip line is very common because of its simplicity and it is not expensive.

1.5. S Parameters

S parameters (S parameters) are used to express the behaviour of Linear Electrical Circuits. They are important in the case of microwave and RF circuits. It gives the relative amplitude and power of a signal at different ports of a network.
In two-port networks, there will be four S parameters namely, S_{11}, S_{12}, S_{21} and S_{22}. The parameters S_{11} and S_{22} indicate reflection and S_{12} and S_{21} indicate transmission of power between ports [8,9].
S_{11} – input reflection
S_{21} – forward transmission/gain (port 1 to 2) also referred to as insertion loss.
S_{12} – reverse gain
S_{22} – output reflection

1.6. Voltage Standing Wave Ratio - VSWR

The VSWR denotes the amount of reflected energy when a signal is sent into a system. VSWR should be lower than 2 for a system [18].

1.7. Load to the Phase Shifters

Many electronic components are having different characteristics depending on different control signals. Some of them change capacitance per voltage, and some, resistance.

1.7.1. Variable Capacitance – Varactor Diode/ Varicap

In the reverse bias, Varactor diodes act as variable capacitance [10]. Using varactor diodes as load makes the phase shifter, voltage controllable. The range of capacitance varies from 1 pF to 30 pF for the BB640 varactor diode [11].

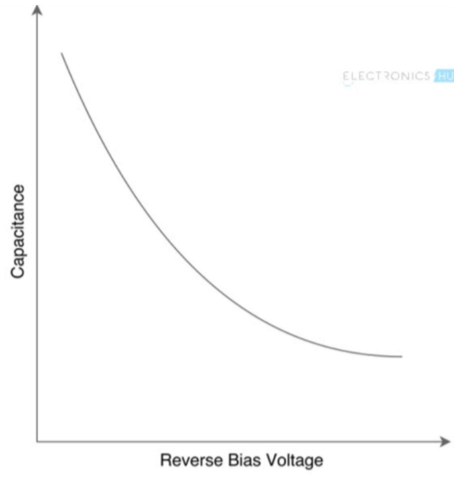

Fig. 9. Reverse Bias Voltage-Capacitance relationship of Varactor diode [10]

Varactor diodes are used in antenna applications [39]. The varactor diode mentioned in [22,39] varies the capacitance between 2.2 pF and 0.3 pF for 0 V - 20 V change in the voltage in the reverse bias. Inductance in series is 0.7nH. The resistance in series is 4.8 Ω.

1.7.2. Variable Resistance - PIN Diode

With varying forward currents, the forward resistance of a PIN diode variation can be seen in Fig.10. Considering forward bias and reverse bias conditions, the tunability of the resistance is from the 'ohm' to 'kilo ohm' range for PIN diodes which is a huge resistance tuning range [38].

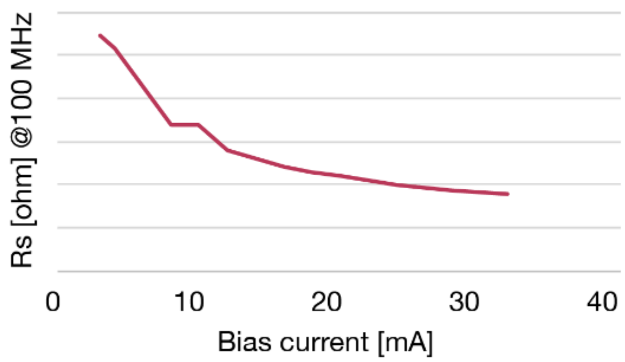

Fig. 10. PIN Diode high-frequency characteristics [12]

PIN diode load to the phase shifters can be realised by varying the resistance at the load while designing.

1.8. Design methodologies of Phase Shifters

1.8.1. Coupler design

90-degree branch line coupler is an important part of the design of the phase shifter of reflection type, or the latter is the extension of the former. Hence the coupler design requires much importance.

The basic structure is shown in Fig. 11. Impedances, Z_0= Z_2 = 50 ohms, Z_1 = $Z_0/\sqrt{2}$, $\theta_1 = \theta_2$ = 45 degrees. While having a structure as in Fig. 12 with open stubs at symmetry planes improves bandwidth by 40% [8]. Flat amplitude characteristics are also a plus.

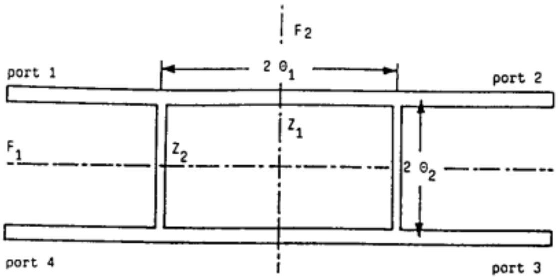

Fig. 11. Symmetrical branch line coupler [8]

A basic branch line coupler is a four-port device as in Fig. 11. It has one input port which is port 1 in the picture. Port 2 is called the through port, port 3 is called the coupled port and the 4 is called the isolation port.

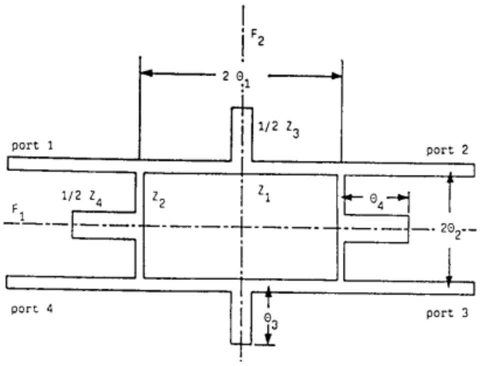

Fig. 12. Coupler design with open stubs [8]

A basic branch line coupler (dual band quadrature coupler) is used in a full duplex, pattern reconfigurable antenna [9], Fig. 14. The structure is shown in Fig. 13 which is the same as Fig. 11.

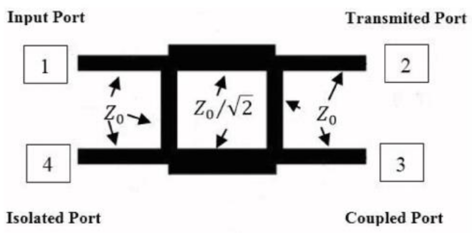

Fig. 13. 3dB branch line couple used in full duplex reconfigurable antenna [9]

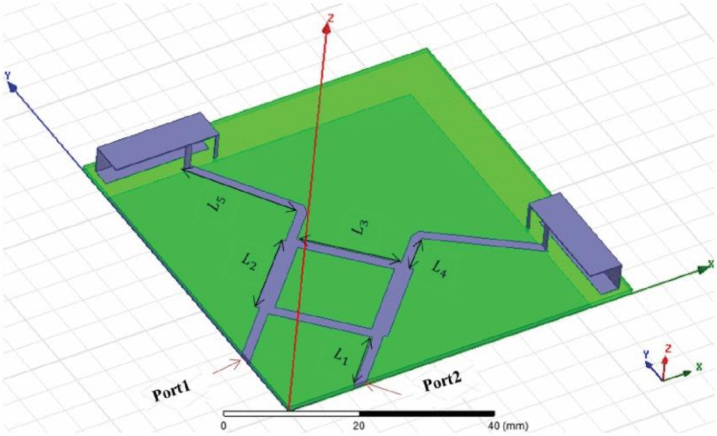

Fig. 14. 2 ×2 MIMO antenna [9]

Multi–stub couplers are discussed in [10]. Improvement in bandwidth is possible to achieve by increasing the number of stubs. The arms are a quarter wavelength long. Designs are shown in Fig. 15.

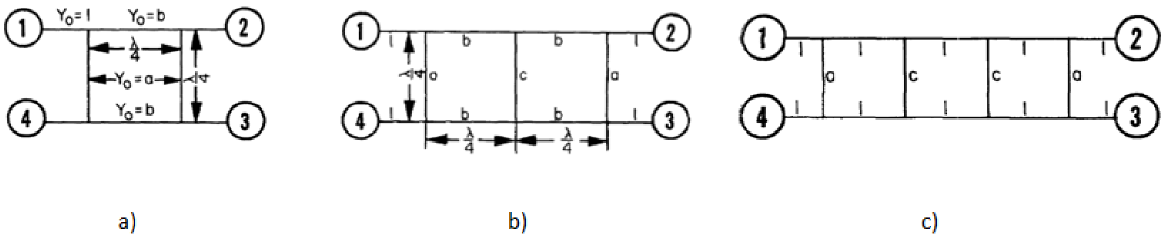

Fig. 15. (a) Single Stub (b) Two Stub (c) Three Stub BLC [10]

For the size reduction of the coupler, a structure called slow wave is used which reduces the phase shifter size and that of the overall antenna system. The branch line coupler is designed using microstrip lines of discontinuous structure [11]. The short and wide line is the capacitive line, and the short and narrow line is the inductive line. This arrangement gives the transmission line a discontinuity (Fig. 16). The S parameters obtained for the design are comparable with that of the conventional coupler design.

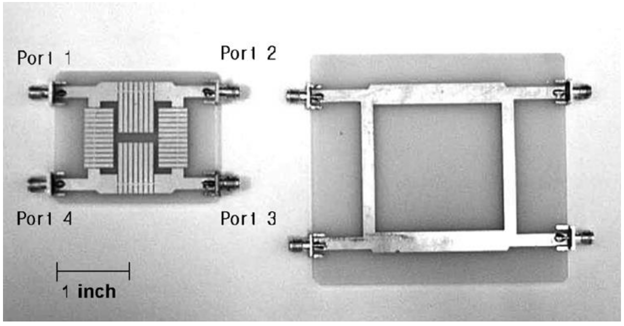

Fig. 16. Left: Coupler with microstrip lines having discontinuity, Right: 3 dB hybrid coupler in a conventional way [11]

For size reduction, the line of quarter wavelength can be seen as a T-model or combinational model (T and π together) and model the branch line coupler accordingly [12]. This approach gives a performance improvement as well. The open stub model is in Fig. 17 (b). The centre frequency is 2.45 GHz and FR4 substrate is used.

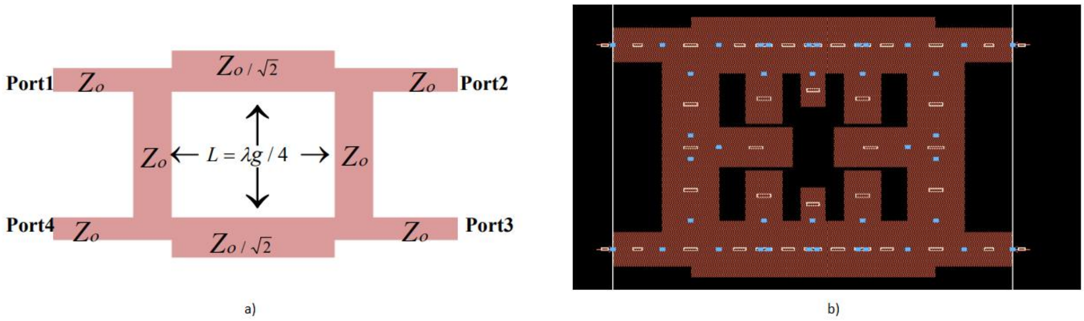

Fig. 17. (a) Conventional 3dB branch line coupler (b) Open stub equivalent [12]

1.9. Phase Shifter Design

A phase shifter is simply the extension of a branch line coupler or any other type of coupler. A low-loss analog phase shifter works at 900 MHz, controlled by a varactor diode is discussed in [13]. The diagram is shown in Fig. 18.

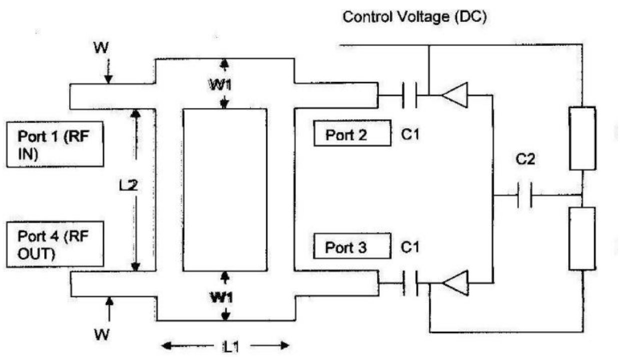

Fig. 18. Varactor-controlled Analog Phase Shifter [13]

In this design, no lumped elements are involved other than to DC bias varactor diode, hence it is scalable according to the frequency requirements. The substrate used is FR4. For a voltage variation of 0 - 32 V DC, a continuous 115 degrees phase shift is obtained. Insertion loss is an average of 1.5 dB which is lower than similar designs.

The advantage of using FR4 substrate is its low cost. [14]. An antenna array is designed using an FR4 substrate as in Fig. 19. Eight dipole slot antenna elements are present in this 5G smartphone antenna. The frequency of operation is 28 GHz.

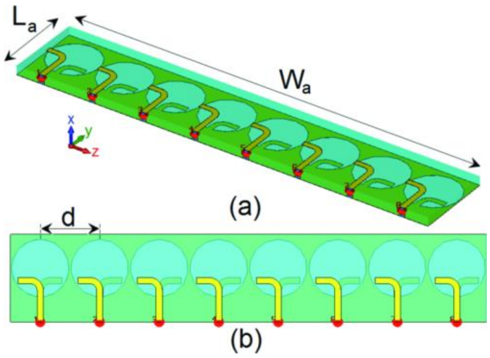

Fig. 19. Schematic of the antenna array. (a) side (b) top views [14]

Some other substrates that can be used [15] are RT5880, RO4350, TMM4, and RO6010. While designing couplers/ phase shifters for higher frequencies for 5G, substrates having low dielectric permittivity and loss tangent (tan δ) with a Q-factor, high is preferred.

For 5G ITS applications (Intelligent Transportation System), bandwidth improvement to the branch line couplers can be achieved with a design as in Fig. 20 (a) [16]. S parameters are as in Fig. 20 (b) and phase in 20 (c).

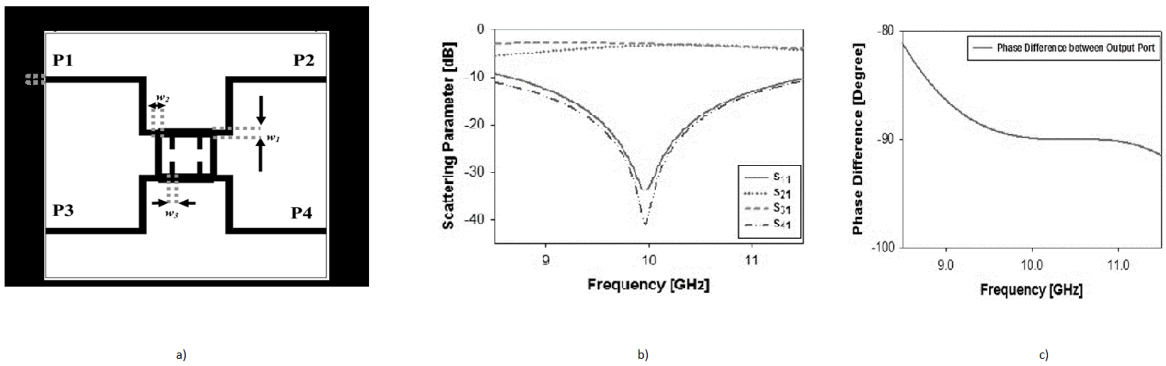

Fig. 20. (a) Coupler design for 5G ITS Applications (b) S parameters (c) Phase difference [16]

This design is based on the stub and slot technique. Enhancement in the bandwidth by up to 60% and improved S parameters and phase differences as compared to conventional design are observed. The operational frequency is 10 GHz and the substrate chosen is Rogers RO4003C.

Reflective load phase shifters with two varactor diodes [17] with independent tuning capabilities have certain advantages. Independent control channels and control algorithms are used for each diode. Compared to the single channel reflective load, the losses are reduced more significantly at higher frequencies hence packaged silicon varactor diodes can replace GaAs components. Different varactor control algorithms are used inside different sub-frequency bands, facilitating bandwidth enhancement. The design is shown in Fig. 21. This design has a total operating bandwidth equal to 10.3% of the available bandwidth and a ripple level of less than 0.8 dB.

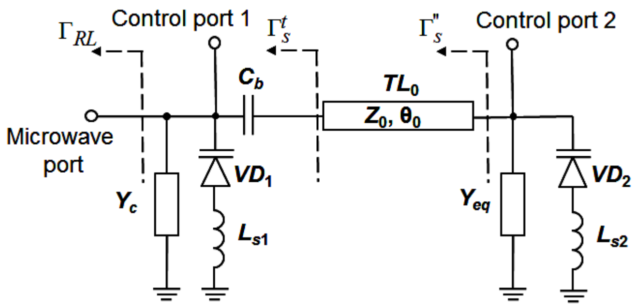

Fig. 21. RL load structure consists of two independent control channels [17]

The compactness of the antenna would be an issue in the millimetre range. 65 nm CMOS technology can be used with small coupled lines. It is suitable for 24 GHz frequency and possible to realise the distributed elements nature such as in above 60 GHz, [18]. Theoretically, massive MIMO antenna modules rely on a dedicated RF chain per antenna element, which is not practical for large arrays. Hence it is important to consider hybrid beam-formers that include both analog and digital phase shifters and find a trade-off between performance, power consumption, and cost.

Self-tuning and closed-loop I/Q generator (Fig. 22) is used in analog phase shifters [19]. A continuous phase shift of 360 degrees is possible and RMS error is minimized in this way. The frequency range is 25 to 30 GHz, hence useful for the 5G technology is the range of 25.5 to 29.5 GHz.

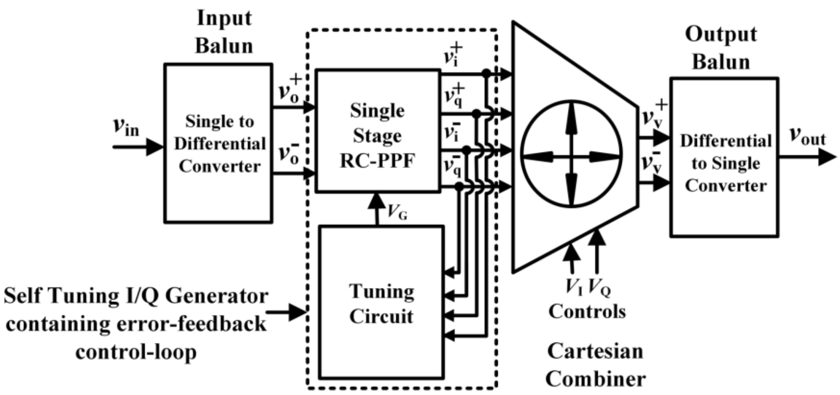

Fig. 22. I/Q generator-based analog phase shifter having self-tuning capability [19]

Reflection-type phase shifters have a low loss. Using a single varactor diode as a load improves the phase response. An open-circuited stub and a varactor diode-loaded stub are parallelly arranged in the load part. Fig. 23. Maximum insertion loss in this way is 2dB [20].

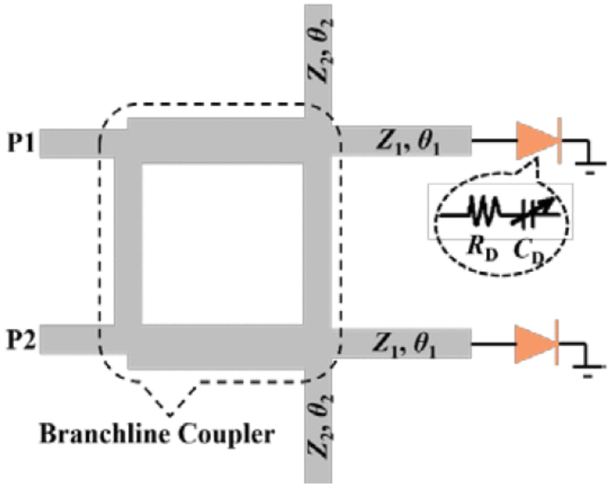

Fig. 23. A single varactor diode load to the reflection-type phase shifter (at 10 GHz) [20]

When the two reflective loads are identical, radio frequency MEMS systems improve the phase shift range [21]. The varactor diodes are thermally actuated, hence contact-based reliability issues are minimized. A low insertion loss, about 5 dB and a phase shift range is 120 degrees are observed here. Frequency 26-30 GHz. Fig. 24.

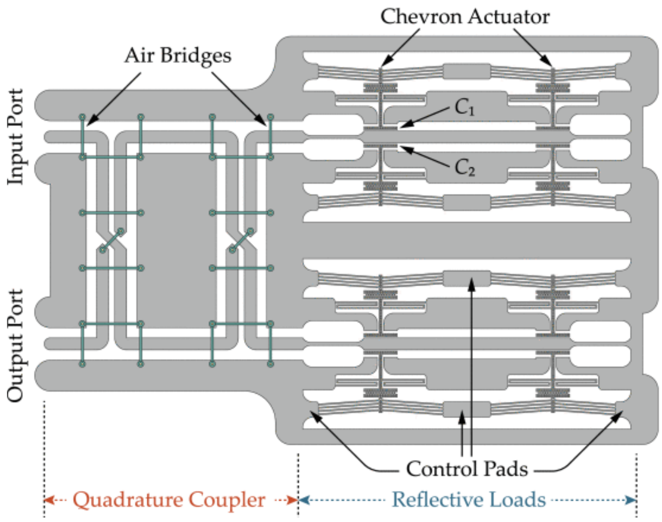

Fig. 24. RTPS layout of tandem quadrature coupler section and two identical reflective loads monolithically integrated [21]

When there are two tunable loads and a tunable capacitor the advantage is that we get a wider bandwidth range (66%) and phase shift tunability and small size [22]. The return loss is 10 dB. The model can be seen in Fig. 25.

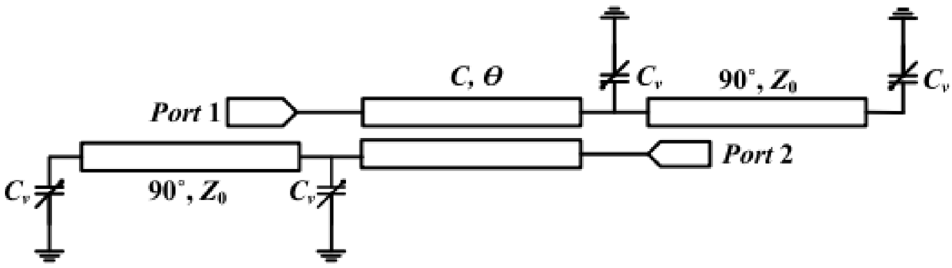

Fig. 25. Reflection-type phase shifter with coupled lines [22]

The result was obtained with a coupler which is planar and vertical. The coupling characteristics of the model are tight over a wide bandwidth and are easily implemented without having small gaps at coupling or extra lumped elements.

In the milli meter range, from 58 GHz to 64 GHz, a phase shifter, passive in nature performs a continuous phase shift over 360 degrees [23]. It has two 90-degree couplers and reflective multi-resonance loads. Size is also compact (Fig. 26). BiCMOS process is followed for design implementation.

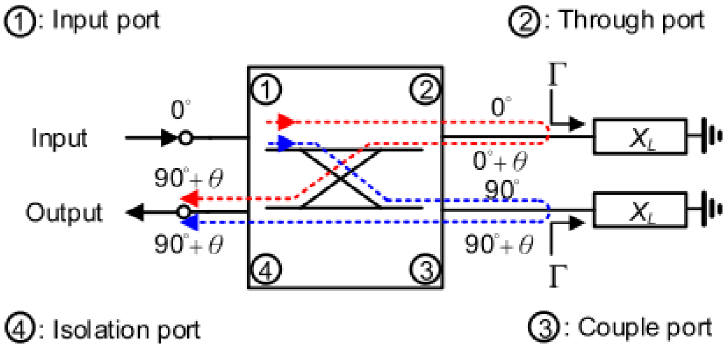

Fig. 26. Reflective type phase shifter with multi-resonant loads [23]

A low error with a phase difference is observed for tunable phase shifters of reflective type [24]. The structure can be seen in Fig. 27. A comparatively low frequency of 2.5 GHz is considered here. Insertion loss is found as low as well.

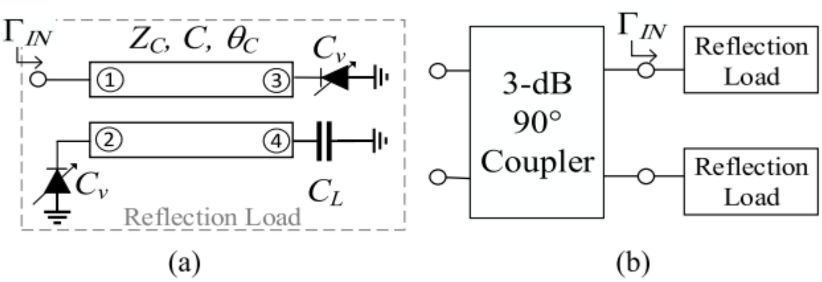

Fig. 27. (a) Reflection load at one port (b) Phase shifter [24]

PIN diode as a load-to-phase shifter is also an option. For tunable antennas, PIN diodes are being used [25,36], Fig. 28.

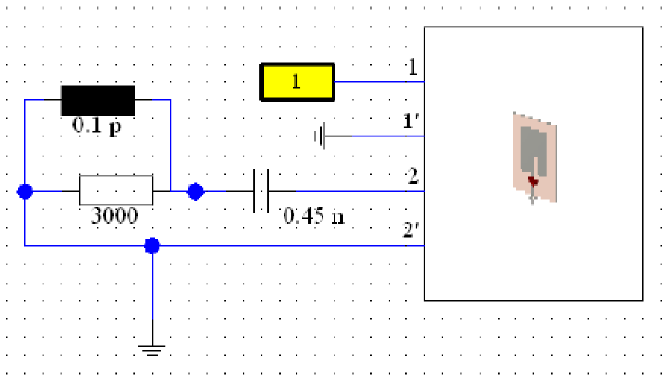

Fig. 28. PIN diode schematic in CST [25]

The behaviour of the phase shifters gets complicated with the load design complexity. Phase shifter designed using substrate integrated waveguide (SIW) – Fig. 29 [26]. Here better phase shift is obtained. Phase shifters can also be designed with varactor diode tunability using SIW [27]. Capacitance variation is 0.09 pF to 1.8 pF with a variation in control voltage between 0 V and 15 V. The operating frequency is 26 GHz. In an antenna design as in [35], for -1 to -8.5 V reverse voltage, the varactor changes its junction capacitance from 1.35 pF to 5 pF [17].

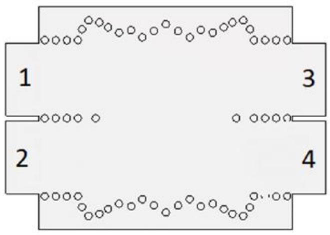

Fig. 29. SIW 3db coupler [26]

Cascaded phase shifters are implemented to improve the overall bandwidth [28]. Two 90-degree hybrid couplers as in the Fig. 30 are used to get a 360-degree reflection-type phase shifter.

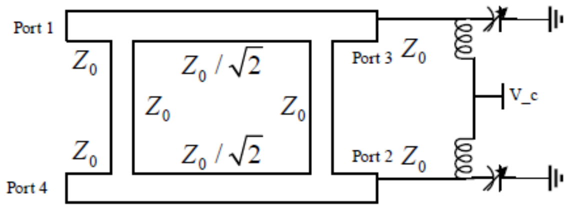

Fig. 30. Single phase shifter in cascaded implementation [28]

Here varactor diode controlled by the voltage of 0-5V range varies the load impedance. 360º phase shift is observed with 2dB insertion loss variation in 3.45 to 3.55 GHz frequency.

Tunable load is the key while dealing with phase shifters. Creative load design can improve bandwidth performances and reduce losses. Fig. 31 (a) shows the dual-band and phase shifter and (b) the load [29].

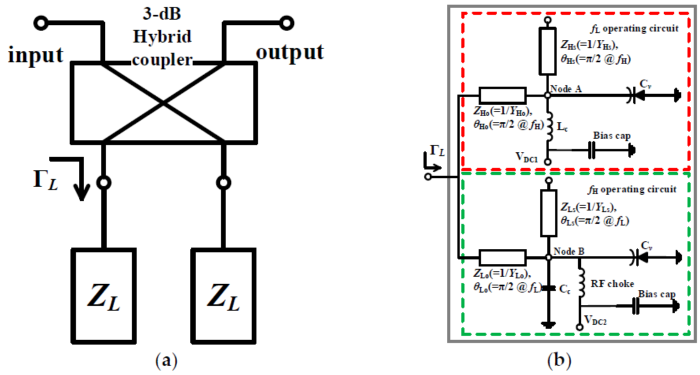

Fig. 31. (a) Phase shifter (b) Load at one port [29]

Here lower working frequency is 1.88 GHz and the higher is 2.44 GHz. Phase shift range and in-band phase deviation are 114.1, 8.43 and 114.0, 5.409 degrees for lower and upper frequencies. Insertion losses are smaller than 1.9 dB and return losses are higher than 16 dB implicating a good performance.

Connecting load after a high impedance line can introduce an additional inductive part to the load overall and becomes a reflective LC circuit (Fig. 32) with the varactor part [30]. In such a way, a better phase shift is achievable for a narrow tunable capacitance range.

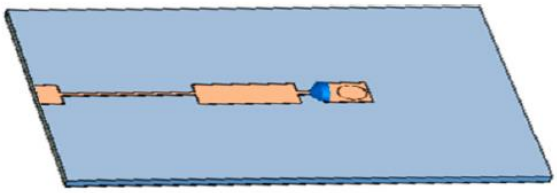

Fig. 32. Reflective LC load [30]

Two such phase shifters combined can give better bandwidth as well. Three directional couplers instead of one or two can give a significant improvement in phase [31]. The model is shown in Fig. 33.

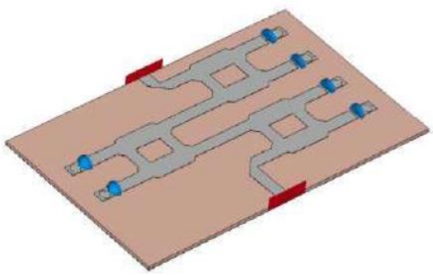

Fig. 33. Phase Shifter design with three BLC [31]

A similar approach as in [30] is mentioned in [32]. Also, a pi-type load design. Another complicated load design is mentioned in [33] which gives bandwidth improvement for phase reference distribution system (PRDS) at 3 GHz working frequency (Fig. 34).

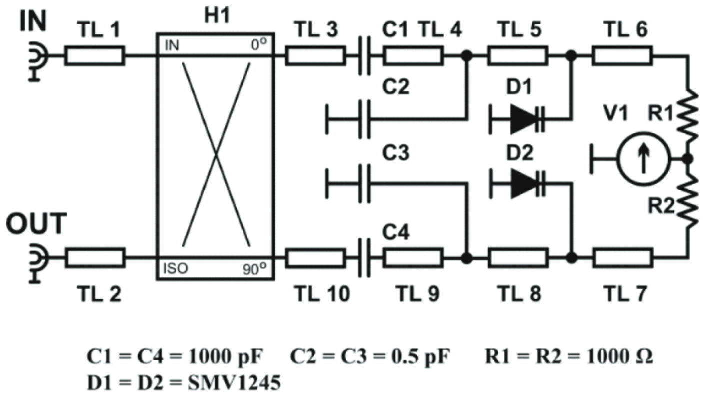

Fig. 34. Current controlled Phase Shifter Design [33]

Most commonly the tunable load being used in phase shifters are varactor diodes. But the capacitance load range is limited to the varactor diode tunable range. So, the available phase shift with constant amplitude is also limited. For this scenario, a digital part is added to the design as a control element to control the varactor diodes [37]. At 26 GHz, around 70 degrees phase shift is achievable in this design.

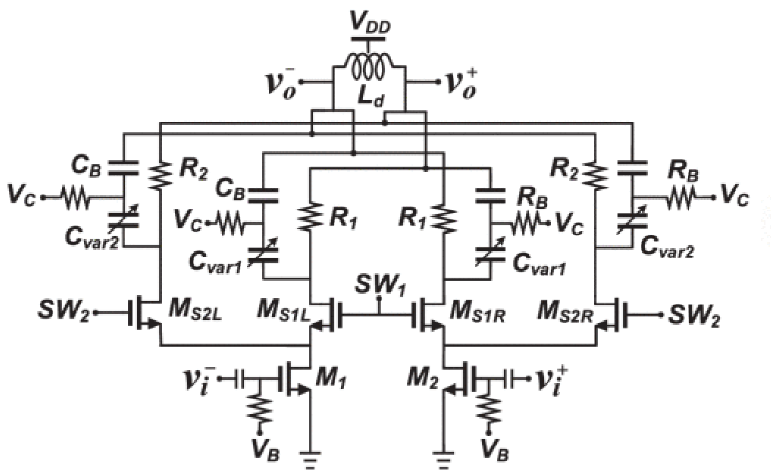

Fig. 35. Phase Shifter model with varactor diode and digital control switch [37]

Phase shifter design varies according to the specific application requirements. Design complexity is acceptable if the phase shift obtained is large enough. The operation bandwidth and size or area of the overall design are also considered while modelling.

The simplest implementation of a phase shifter is using a 3 dB branch-line coupler. It has a simple planar structure, and the fabrication is easy and can be done on the same PCB. Variable load to a basic coupler structure is where the comparison study begins, and different design varieties can be tried.

2. Modeling

2.1. Calculation of Parameters

A 3 dB coupler is an inevitable part of the design. While dealing with microwaves, couplers are for splitting or joining the power of the input signal the way according to the application requirements by changing the port at which we give input and isolation.

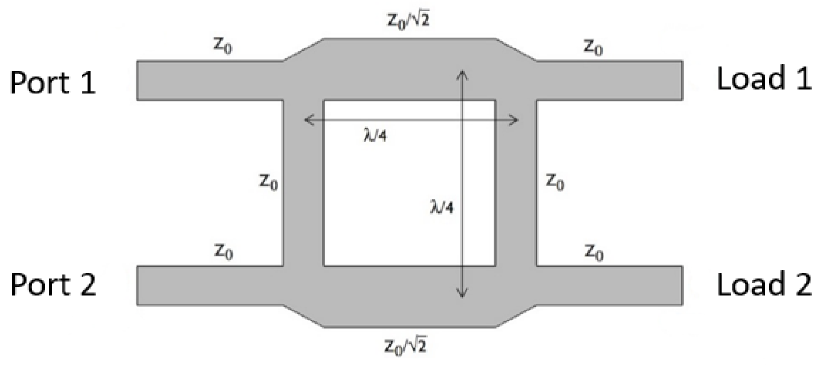

Fig. 36. Reflection type phase shifter with single section 90-degree hybrid coupler [13]

We fix the substrate height, trace the thickness and impedance of the line and find the stripline width and quarter wavelength which we use in the design. The below-mentioned equations [40,41] are being used. A PCB layout is prepared based on the micro-stripline feeding technique with the line length and width obtained from the calculations. The width of the strip lines increases with decreasing line impedance.

The microstrip patch width is represented by w which is calculated using equation (1).

$$w = \frac{c}{2f_r}\sqrt{\frac{2}{\varepsilon_r + 1}} \tag{1}$$

C – Speed of light
Fr – Frequency of Resonance
ε_r – dielectric constant of the substrate(FR4) [40]

The effective dielectric constant of the microstrip line is calculated using equation (2).

$$\varepsilon_{eff} = \frac{\varepsilon_r + 1}{2} + \frac{\varepsilon_r - 1}{2}\left(1 + \frac{12h}{w}\right)^{\frac{-1}{2}} \tag{2}$$

h- Height of substrate [40]

The effective length of the patch is given as,

$$L_{eff} = \frac{c}{2f_r\sqrt{\epsilon_{eff}}} \quad (3)$$

The actual length of the patch is given as,

$$L = L_{eff} - \Delta L \quad (4)$$

The factor ΔL is [40],

$$\Delta L = 0.412h\frac{(\epsilon_r + 0.3)(\frac{w}{h} + 0.264)}{(\epsilon_r - 0.258)(\frac{w}{h} + 0.8)} \quad (5)$$

2.2. The Effect of Dimensions

While dealing with high frequencies, the dimensions of the design get reduced because of the quarter-wavelength-based development of the model. The substrate height is 1mm, and the patch thickness is 36 µm. The width of the 50 Ohms line is 2 mm. The width of the 35 Ohms line is 3.3 mm. The

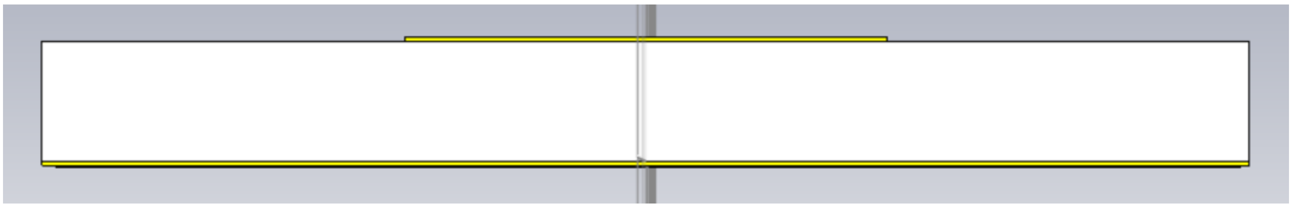

Fig. 37. Microstripline feeding

obtained quarter wavelength is 11.6 mm. Line length is particularly important. Considering the quarter wavelength from centre to centre of our thick transmission lines, the results we get are different compared to the results where we take the quarter wavelength from corner to corner.

2.3. 3D Modeling and S Parameters

2.3.1. The Coupler

The coupler design has been done using the calculations mentioned in the Modeling. Necessary modifications are done with the line length so that the operating frequency is 3500 MHz. 3Dthe Model is shown in Fig. 38 and S parameters are as in Fig. 39 and 40.

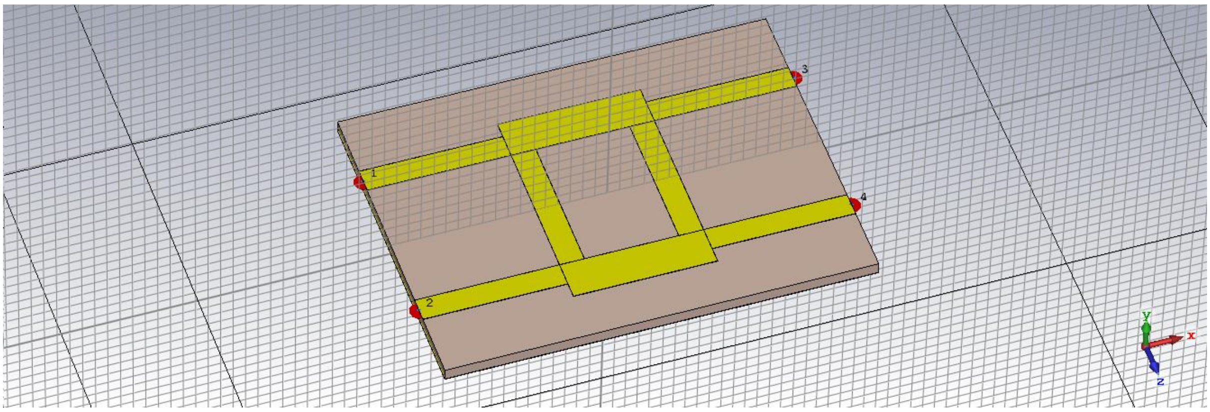

Fig. 38. 3D Model of the 3 dB Branchline Coupler with a single section

S_{11} and S_{21} are higher than -15 dB. It implies that there is less reflection in port 1 and less power transfer to port 2 which is the isolation port in this case. S_{31} and S_{41} nearly -3 dB means that the input power splits equally to ports 3 and 4. Hence the coupler design is verified working and can be used to build a phase shifter.

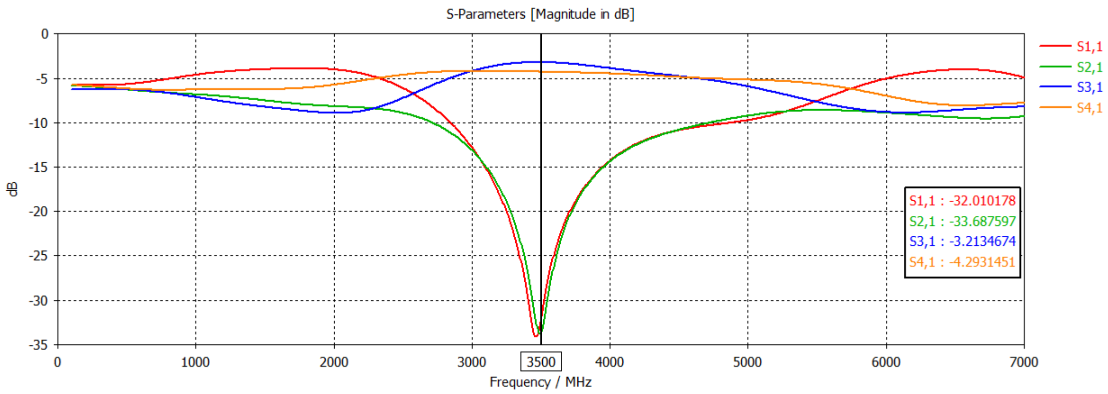

Fig. 39. S parameters of the coupler the 3 dB Branchline Coupler with a single section

The phase difference between ports 3 and 4 should be 90 degrees at the working frequency. It has been checked and verified to be 90 degrees (90.34). Fig. 40 shows this difference.

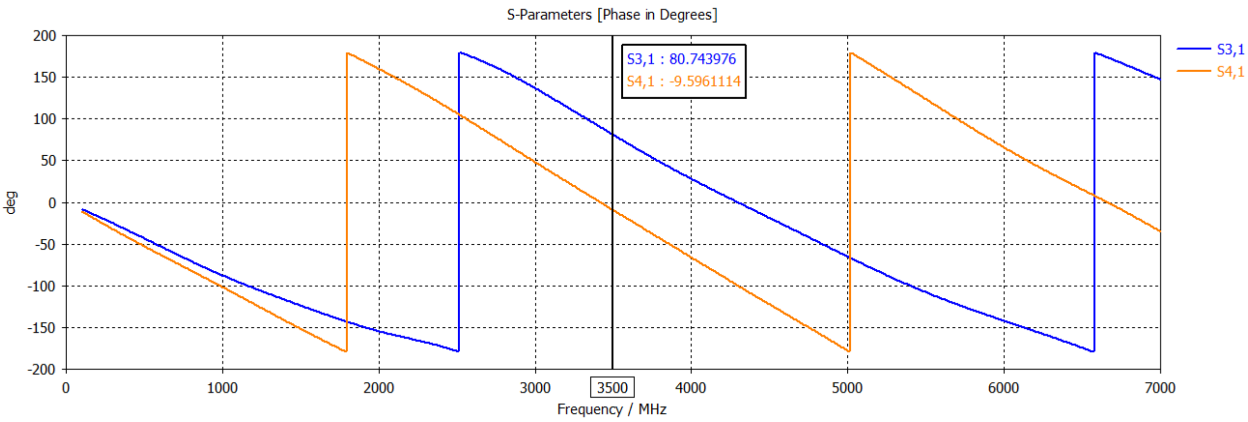

Fig. 40. Shift in phase between port 3 and port 4 of the BLC

Similar to the basic BLC with a single section, two sections of BLC are designed and verified [19]. Bandwidth improvement is observed around the operating frequency. The model and S parameters are shown in Fig. 41 and Fig. 42.

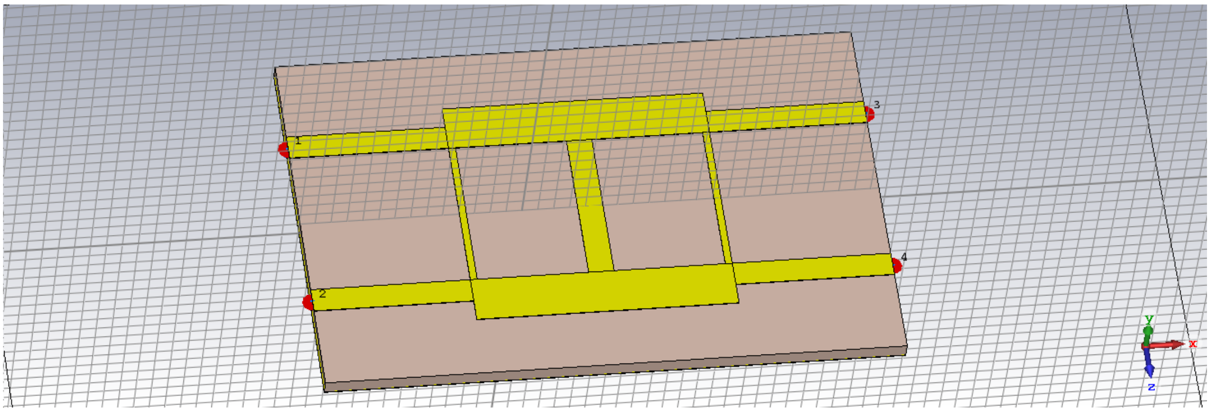

Fig. 41. 3D Model of the 3 dB BLC with two sections

In Fig. 41, the improved bandwidth performance is shown. Two operating frequencies are found instead of one as 3.5 GHz and 5.25 GHz.

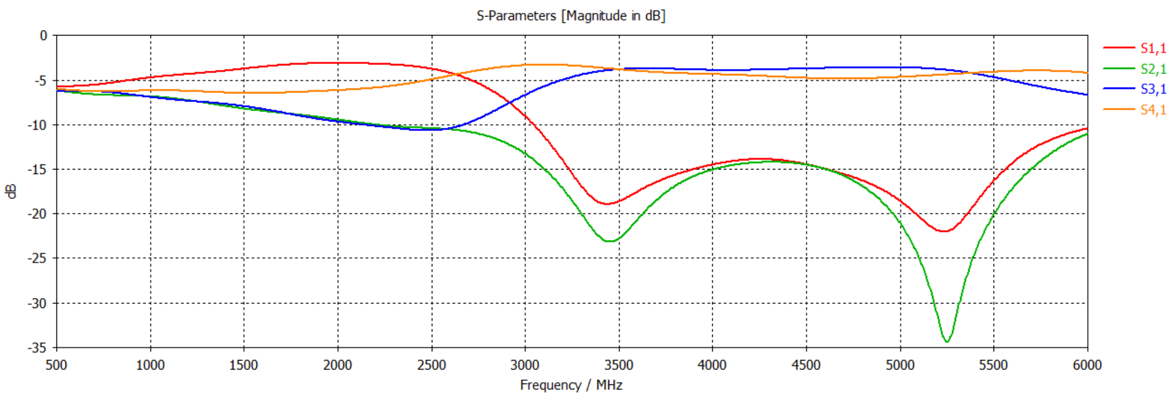

Fig. 42. S parameters of the 3 dB BLC with two sections

2.3.2. Phase Shifter – Single Section

Single section phase shifter is obtained by loading port 3 and port 4 of the coupler designed in Fig.37. Here the varactor realisation has been done by varying the capacitance load from 1 pF to 10 pF. For that purpose, lumped element option in CST has been used. For better stability and low loss, both loads are kept the same. Fig. 43 shows the 3D model, Fig. 44 and Fig. 45 show the S parameters, Fig. 46 shows the phase and Fig. 47 shows the VSWR.

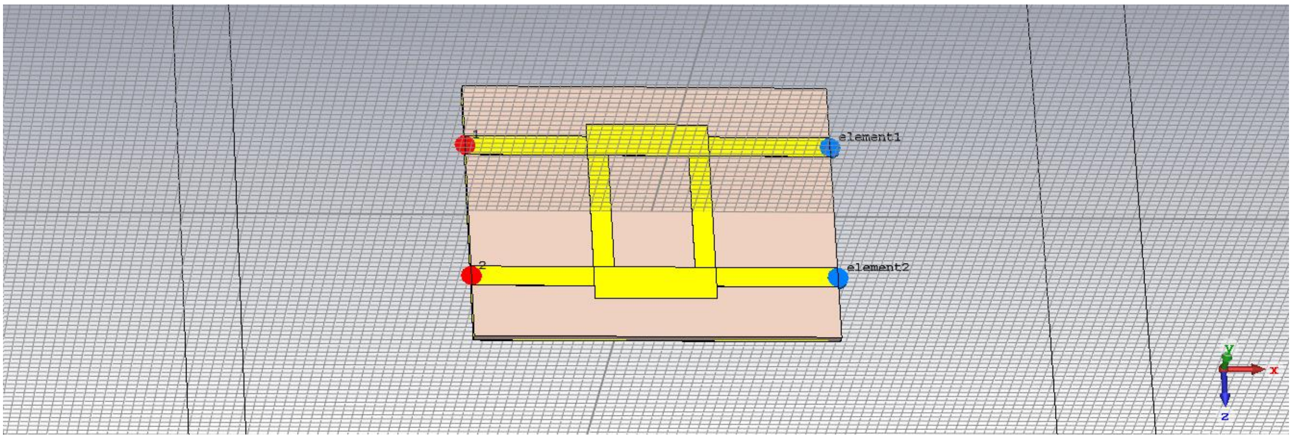

Fig. 43. Single section BLC phase shifter – 3D Model

The input port reflections are more negative than -15 dB indicating a good matching as shown in Fig. 44. In single-section coupler-based phase shifter design, wider bandwidth is not usually observed. Here we are observing minimum values at two frequencies around 3300 MHz and 3700 MHz. Throughout this range, the S_{11} value is also desirable. It can be because the phase shifter dimensions are based on a small quarter wavelength.

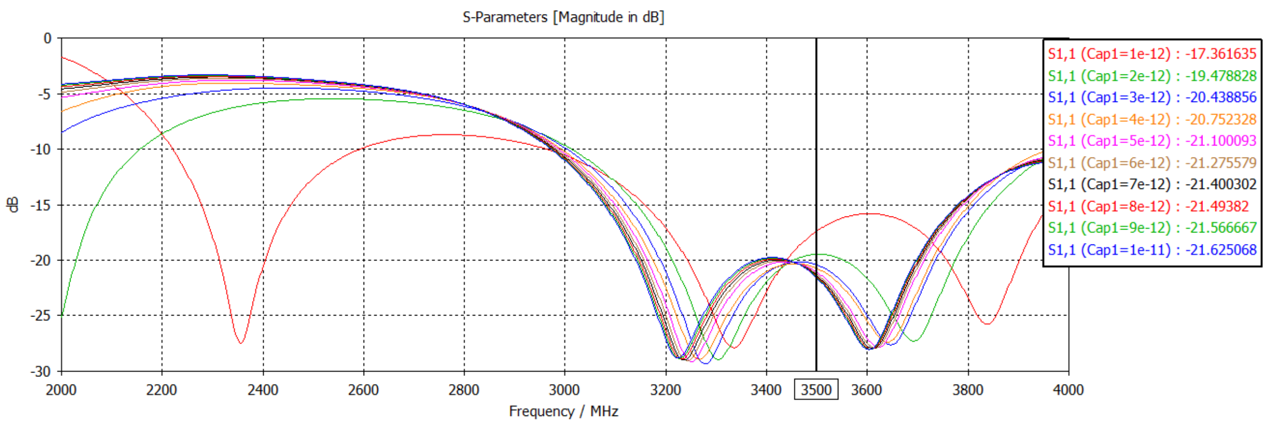

Fig. 44. Single section BLC phase shifter - Input port Reflection, S_{11} in dB

The insertion loss is observed to be around -1.5 dB for all values of capacitance for this model. It is shown in Fig. 45.

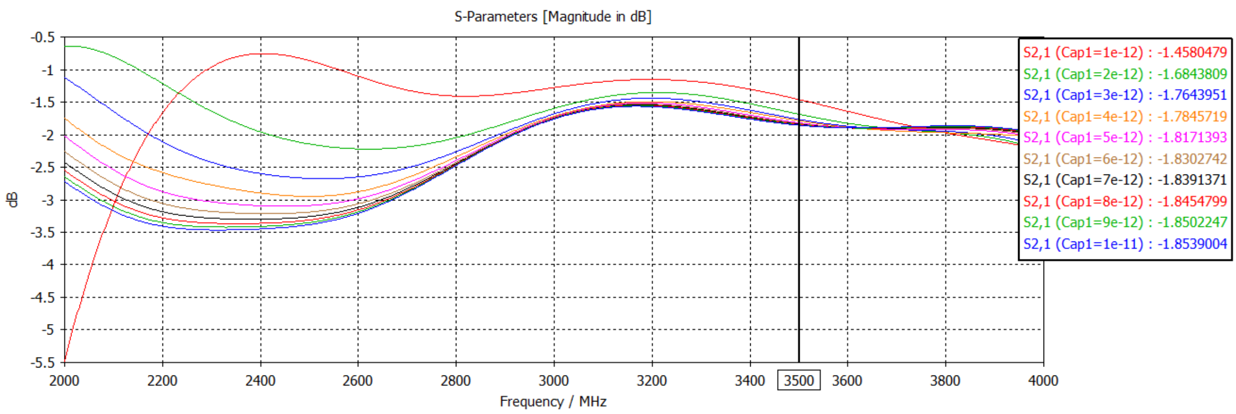

Fig. 45. Single section BLC phase shifter - Insertion loss, S_{21} in dB

The phase shift observed at port 2 concerning port 1 is nothing but the phase of the S parameter S_{21}. It has been shown in Fig. 46 for this model.

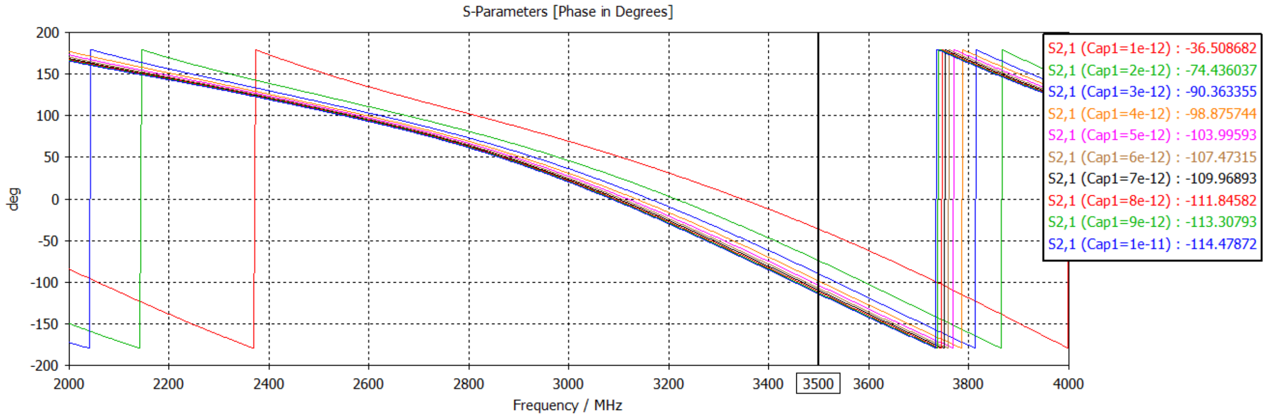

Fig. 46. Single section BLC phase shifter - phase of S_{21} in degrees

VSWR at both ports 1 and 2 is smaller than 2 as shown in Fig. 47.

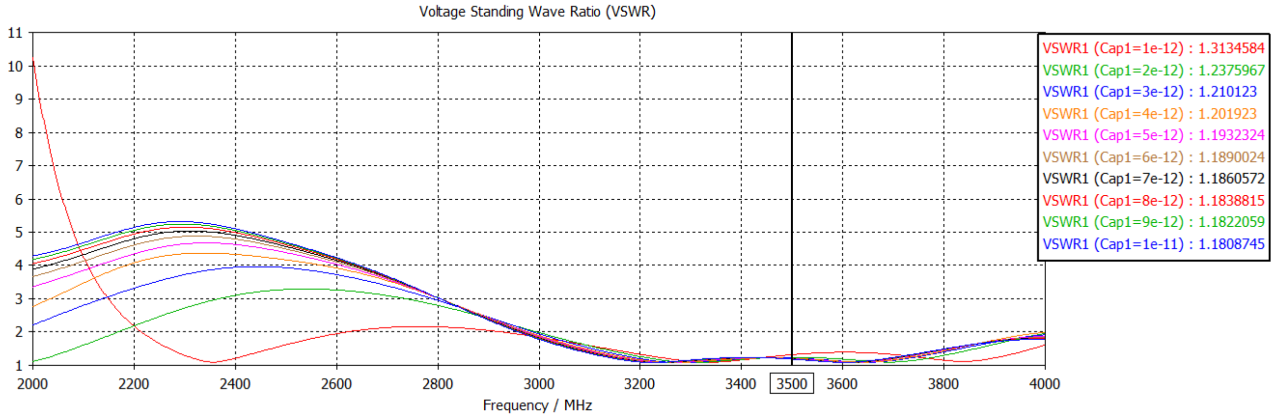

Fig. 47. Single section BLC phase shifter - VSWR

For PIN diode realisation, the resistance of the lumped element is varied from 10 ohms to 100 ohms. In this model, a very high insertion loss is observed. Fig. 48 and Fig 49 show the S parameters and Fig. 50 shows the phase for this case. S_{11} values are acceptable and it is showing a narrow band behaviour as in Fig. 48.

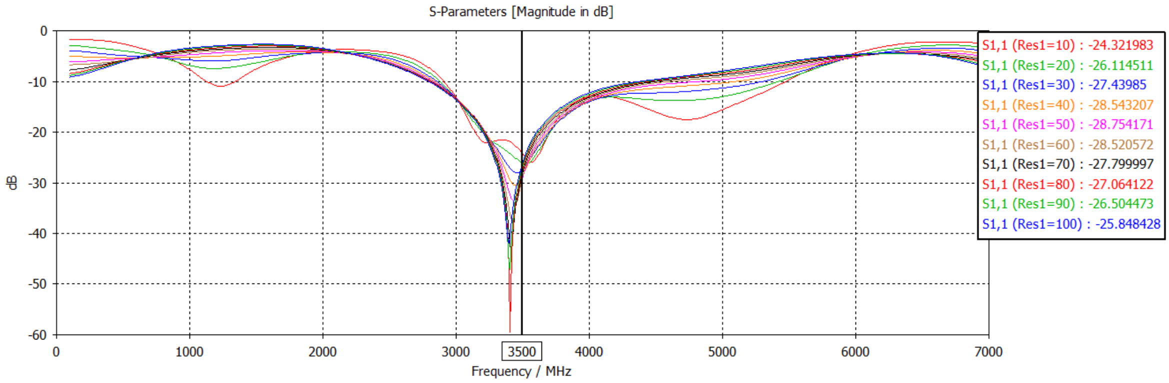

Fig. 48. Single section BLC phase shifter with PIN diode load - Input port Reflection, S_{11} in dB

The insertion loss is not in the acceptable range for this case and this model. It is shown in Fig. 49.

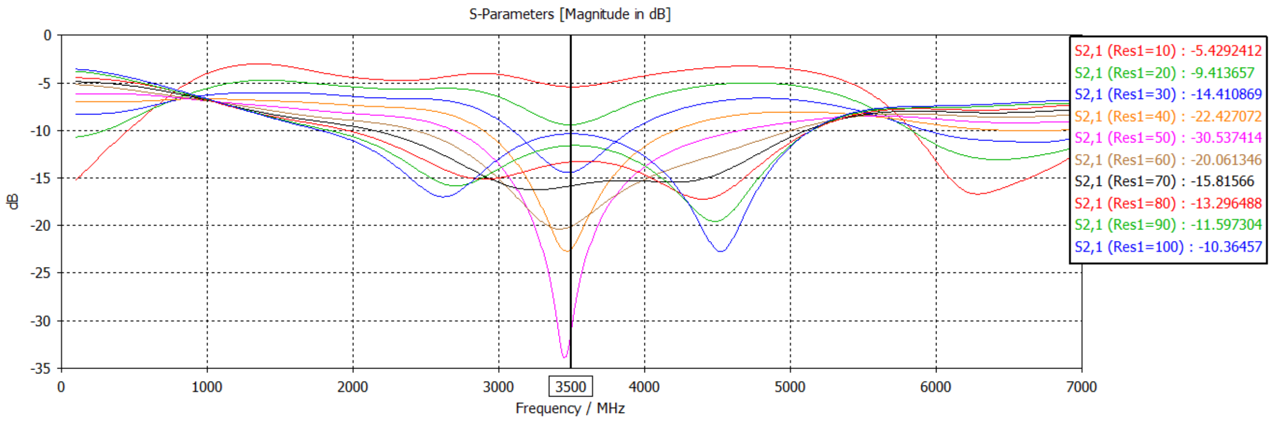

Fig. 49. Single section BLC phase shifter with PIN diode load - Insertion loss, S_{21} in dB

The phase shift characteristics are not stable as well for this case also not very significant.

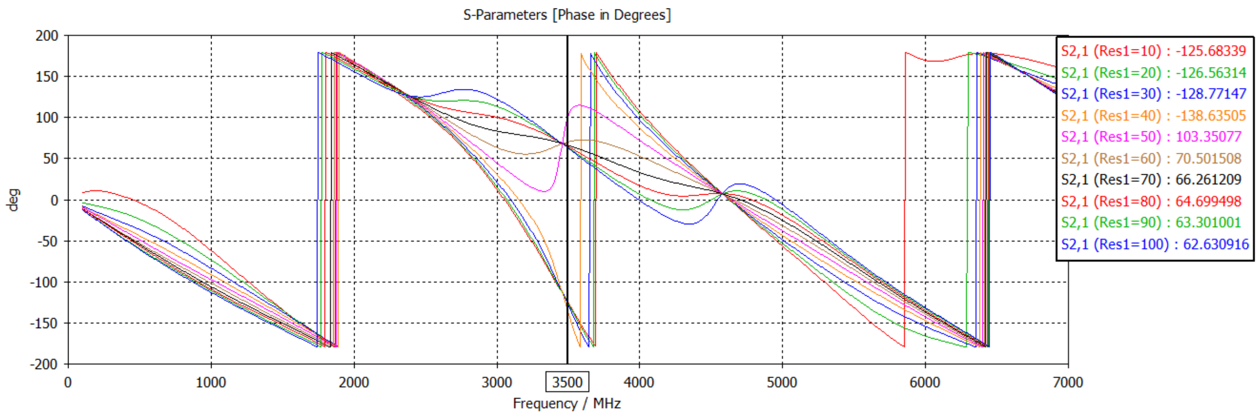

Fig. 50. Single section BLC phase shifter with PIN diode load - phase of S_{21} in degrees

2.3.3. Phase Shifter with Two-Section BLC

For the bandwidth improvement purpose, a two-section BLC is modelled. The varactor diode load realisation has been done as done on the phase shifter with a single section BLC. Fig. 49 shows the 3D model of the design, Fig. 51 and Fig. 52 shows S parameters, Fig. 53 shows the phase and Fig.54 shows VSWR1.

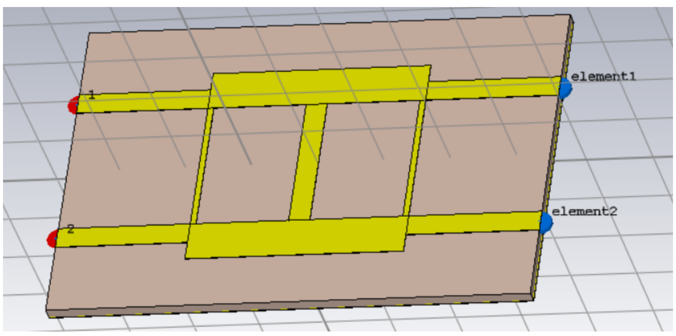

Fig. 51. Two sections BLC phase shifter – 3D Model

The reflection losses are similar to the first design with varactor load. The bandwidth improvement has been observed for the coupler design with two sections on which this model has been developed. The minimum values of S_{11} are found at two frequencies as in the coupler part.

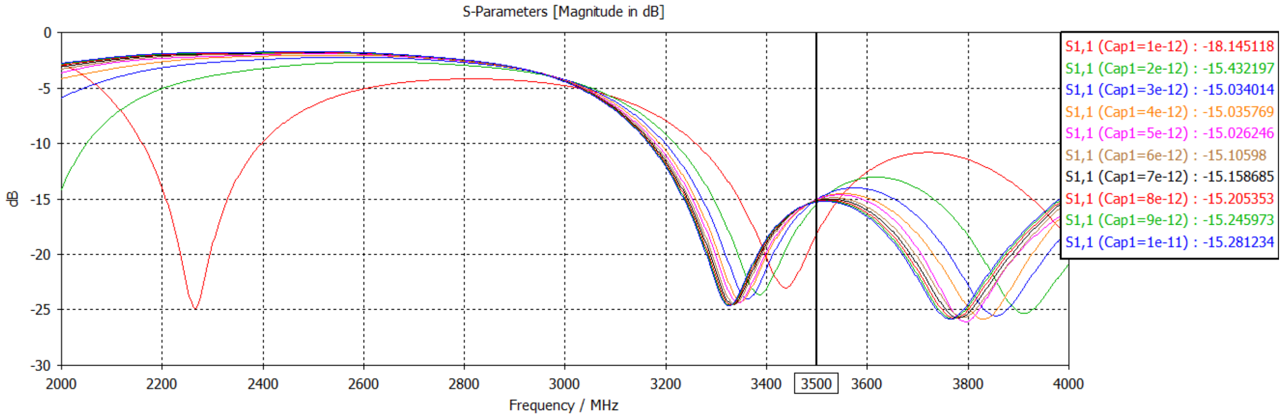

Fig. 52. Two sections BLC phase shifter - Input port Reflection, S_{11} in dB

Insertion losses are in the acceptable range as in Fig. 53.

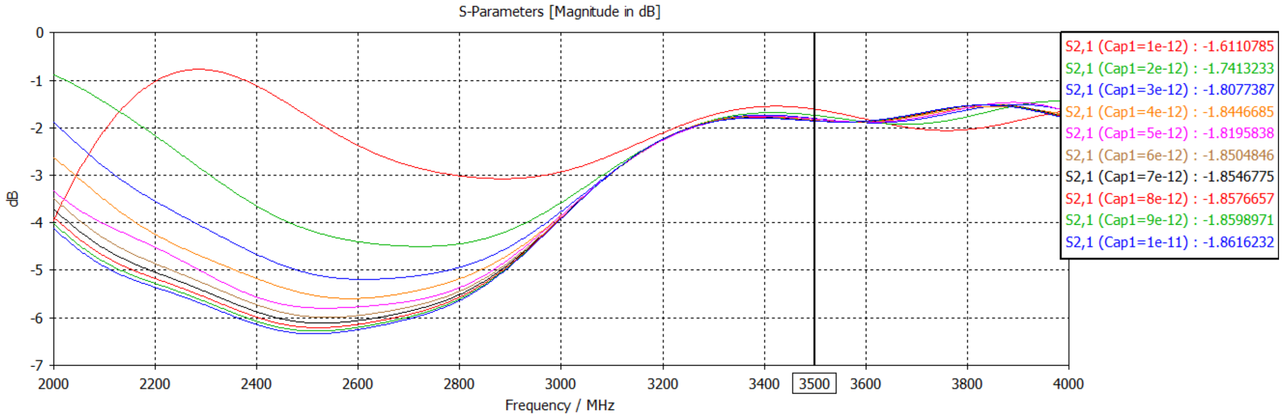

Fig. 53. Two sections BLC phase shifter - Insertion loss, S_{21} in dB

Phase shows a very stable variation over the C band frequencies for this case as in Fig. 54.

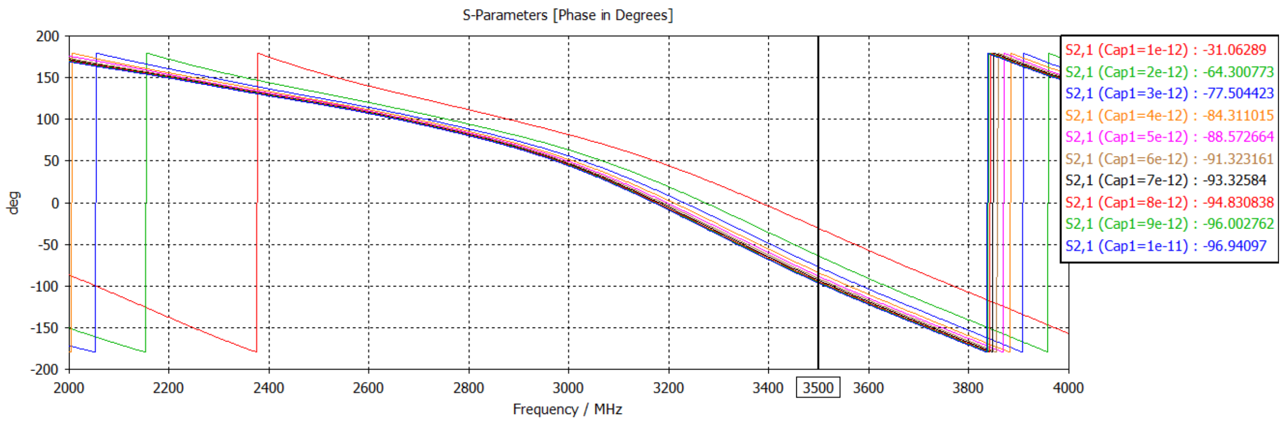

Fig. 54. Two sections BLC phase shifter - phase of S_{21} in degrees

VSWR is small and acceptable as shown in Fig. 55.

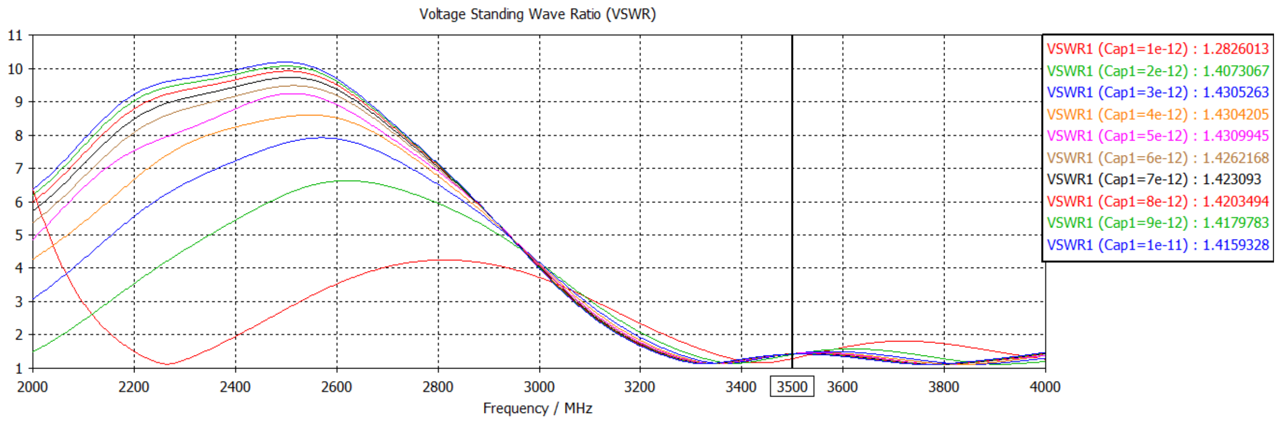

Fig. 55. Two sections BLC phase shifter – VSWR

2.3.4. Phase Shifter with a high impedance line before the load

To improve the phase shift, the load part has been modified so that there is a high-impedance line before the load. Fig. 56 shows the design, Fig. 57 and 58 show the S parameters, Fig. 59 shows the phase of this design and Fig. 60 shows the VSWR.

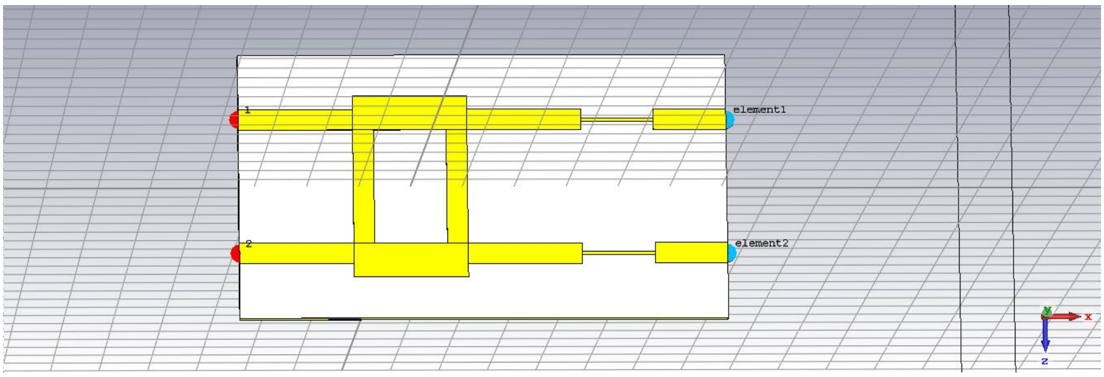

Fig. 56. Phase Shifter with a high impedance line before the load - 3D Model

The minimum values are found at the frequency 3500 MHz. The losses are in a similar range as those of the previous designs.

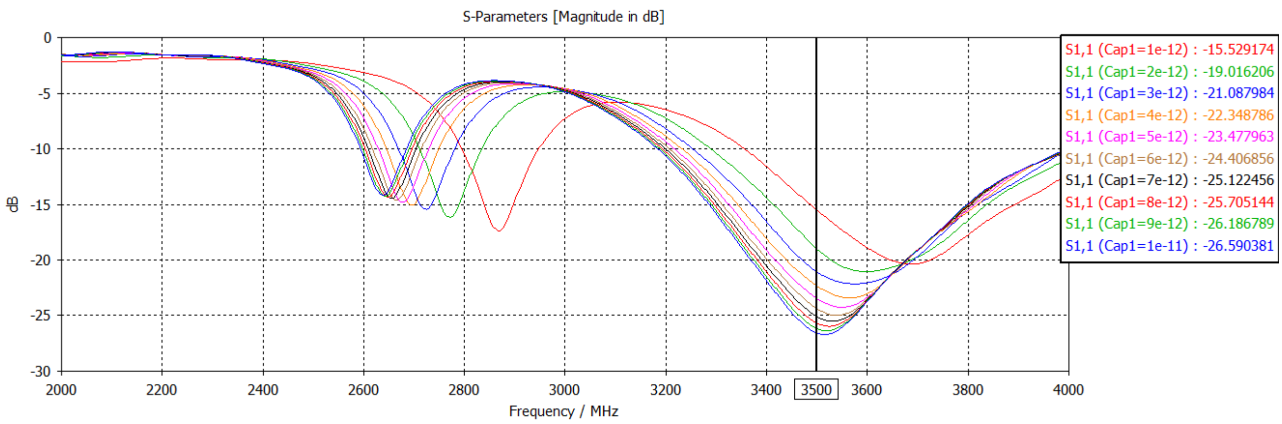

Fig. 57. Phase Shifter with a high impedance line before the load - Input port Reflection, S_{11} in dB

Insertion loss, S_{21} is than -2 dB. It is shown in Fig. 58.

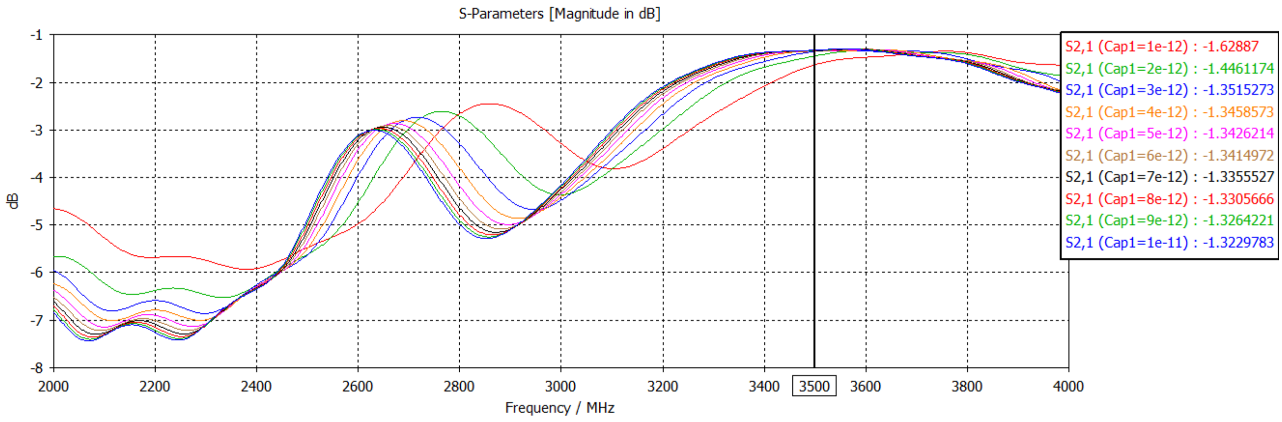

Fig. 58. Phase Shifter with a high impedance line before the load - Insertion loss, S_{21} in dB

The phase shift obtained is less compared to the previous designs as shown in Fig. 59.

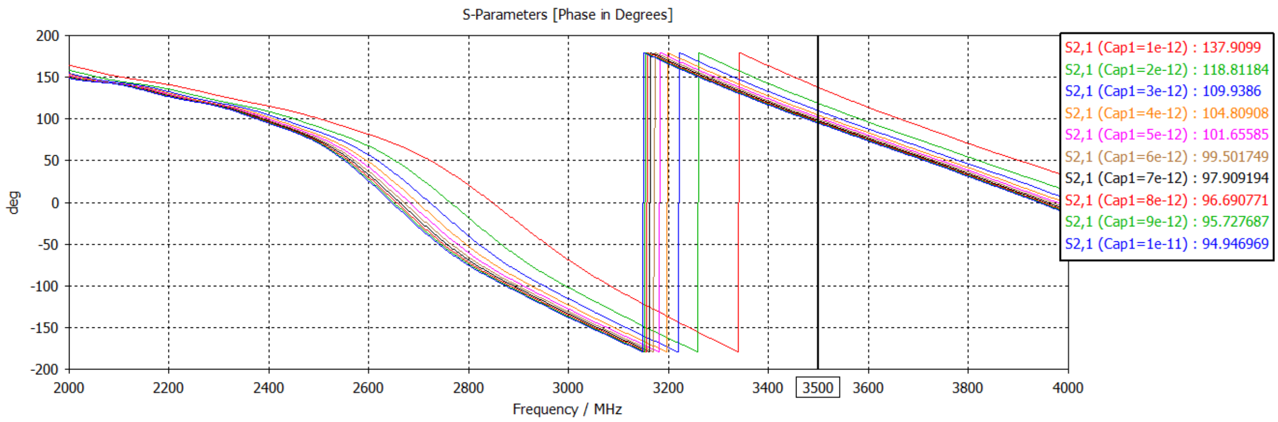

Fig. 59. Phase Shifter with a high impedance line before the load - phase of S_{21} in degrees

VSWR is less than 2 in the operating frequency as shown in Fig. 60.

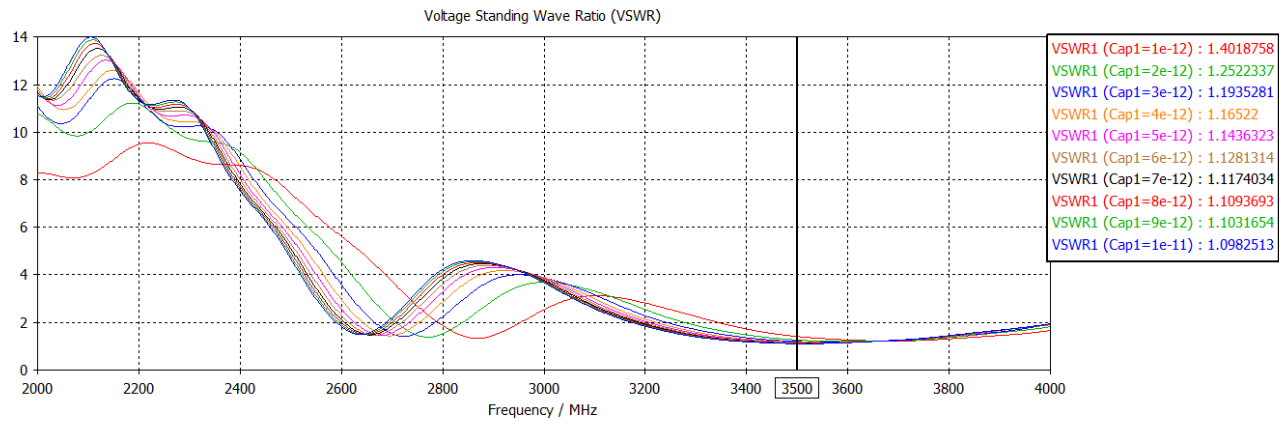

Fig. 60. Phase Shifter with a high impedance line before the load – VSWR

2.3.5. Influence of line length, Width and Height of Substrate

While implementing the model, there is a possibility for changes in the length or width of the stripline or the height of the substrate. It can cause variations in the frequency of operation and affect the losses. On the first model of the phase shifter with a single section BLC, alteration of these three parameters is done and observed the results.

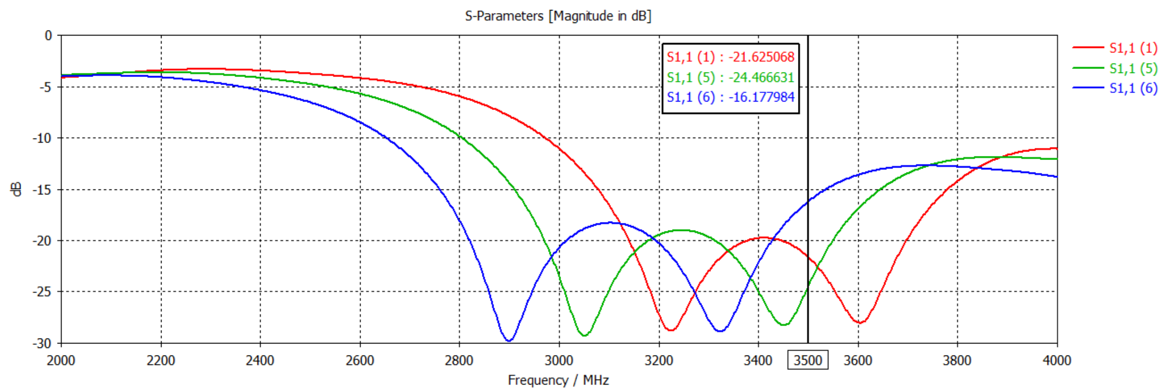

Fig. 61. S_{11} when the length of the line varies

In Fig. 61 when the length is increased by 10%, the operating frequency is shifted by 127 MHz to the left, thus the frequency is reduced. When the increment is 20%, the shift is 224 MHz.

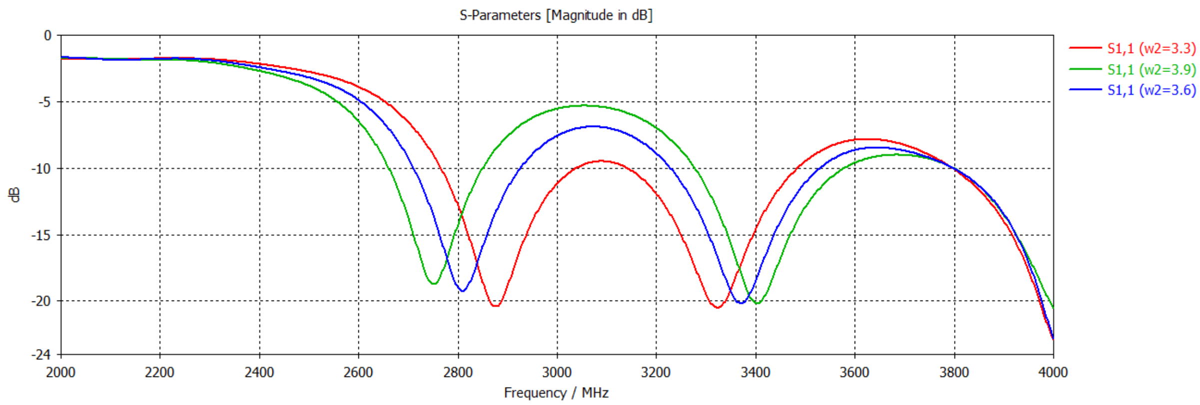

Fig. 62. S_{11} when the width of the line varies

When the width of the line with an impedance $Z_0/\sqrt{2}$ is varied, the results are shown in Fig. 62. When the width increased by 10%, the operating frequency shifted by 31 MHz to the left. When the width increases by 20%, the shift is 78 MHz to the left.

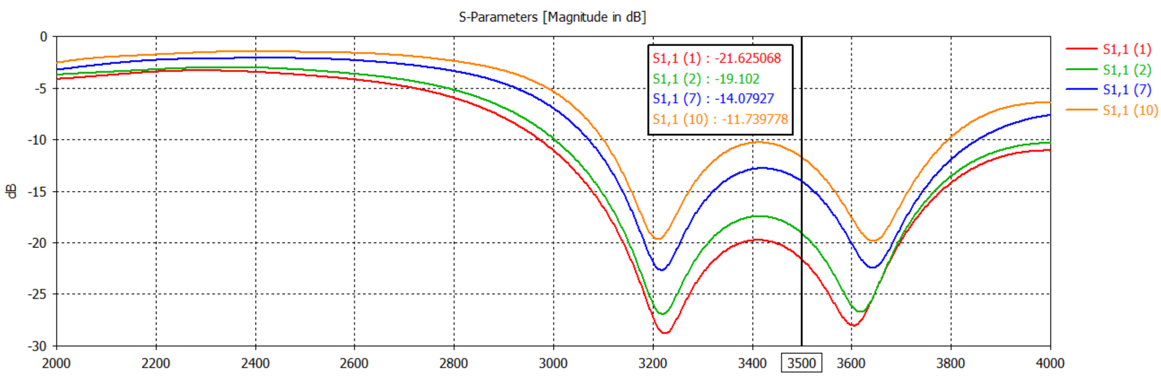

Fig. 63. S_{11} when the height of the substrate varies

When the substrate height varies, it affects losses. It does not have much effect on the operating frequency. Fig. 63 shows that the reflection coefficient is moving upwards with an increase in the substrate height. When the height increased by 10%, the S11 is in the allowed range but when increased by 50% and when doubled the height, the S11 values are not acceptable.

3. Results and Discussions

Phase shift vs varying capacitance graphs are plotted for all three models. A linear phase variation with frequency is observed in every model. The models show similar phase tunability with the capacitance variation.

For the first model, the phase shift against the varying capacitance value can be seen in Fig. 64 which is not linear. The slope is maximum indicating that the phase shift is maximum between 1 pF and 2 pF followed by the 2 pF to 3 pF range. After 3 pF the phase shift with varying capacitance is reduced.

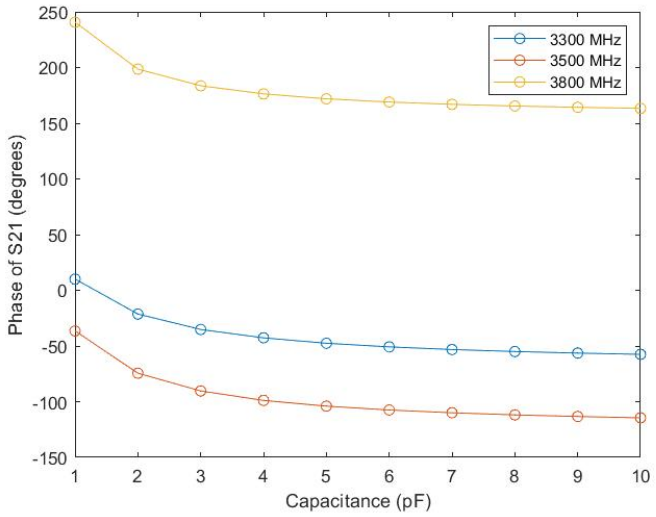

Fig. 64. Phase Shift vs Capacitance – Phase shifter with A single section BLC

The second model shows that a tunable phase can be achieved using the phase shifter with two sections of BLC in all the measured frequencies (Fig. 65). The behaviour is the same in all observed frequencies.

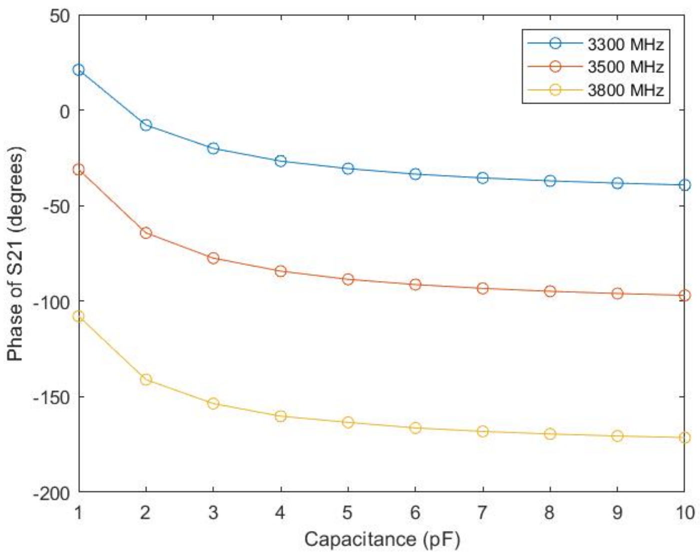

Fig. 65. Phase Shift vs Capacitance – Phase shifter with two sections BLC

For the third model, the slope for these frequencies is smaller compared to the former plots since the phase shift is less (Fig. 66).

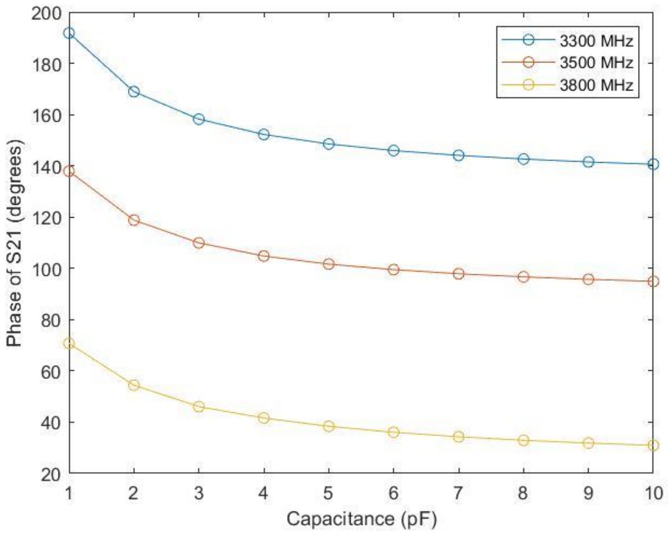

Fig. 66. Phase Shift vs Capacitance – Phase shifter with a high impedance line before the load

The phase shifts and losses are given in Table 2. Considering the loss profile, the phase shifter design with a high impedance line is performing better. Better phase shift is given by the first design with a single section BLC which is the smallest by the dimensions and simplest by the design.

Table 2. Performance Comparison of the Models with varactor load

Model	The magnitude of the Total Available Phase Shift at the Operating Frequency (Degrees)	Average Return Loss in all measured frequencies (dB)	Average Return Loss in the Operating Frequency (dB)	Average Insertion Loss in all measured frequency (dB)	Average Insertion Loss in the Operating Frequency (dB)
Phase shifter with a single-section BLC	77.97	-20.59	-20.65	-1.74	-1.77
Phase shifter with two sections BLC	65.88	-19.27	-15.47	-1.76	-1.81

Phase Shifter with a high impedance line before the load	42.96	-17.28	-22.91	-1.59	-1.38

Conclusions

1. The maximum phase shift was obtained for the first design with a single stub branch line coupler which is 77.97 degrees.
2. Loss performances of the phase shifters are similar to each other and within the allowed range. The third design of the phase shifter with a high impedance line gives an average return loss of -22.9 dB and an average insertion loss of -1.58 dB which is the best among the designs. The phase shift obtained for this design is 42.96 degrees.
3. With the two-section branch-line coupler-based phase shifter design, the phase shift obtained is 65.88 degrees.
4. Even with small dimensions and without a load design complexity, phase shifters can be designed with high performance.
5. At the implementation level, variations in line length, line width and substrate height can change the behaviour of the phase shifter in terms of operating frequency and losses.

List of references

1. Pirinen, Pekka. (2014). A Brief Overview of 5G Research Activities. 10.4108/icst.5gu.2014.258061.
2. Albreem, Mahmoud A. M.. "5G wireless communication systems: Vision and challenges." *2015 International Conference on Computer, Communications, and Control Technology (I4CT)* (2015): 493-497.
3. Attar, Hani H. et al. "5G System Overview for Ongoing Smart Applications: Structure, Requirements, and Specifications." *Computational Intelligence and Neuroscience* 2022 (2022): n. pag.
4. T.E. Bogale, X. Wang, L.B. Le, Chapter 9 - mmWave communication enabling techniques for 5G wireless systems: A link level perspective, Editor(s): Shahid Mumtaz, Jonathan Rodriguez, Linglong Dai, mmWave Massive MIMO, Academic Press, 2017
5. E. Björnson, E. G. Larsson and M. Debbah, "Massive MIMO for Maximal Spectral Efficiency: How Many Users and Pilots Should Be Allocated?," in IEEE Transactions on Wireless Communications, vol. 15, no. 2, pp. 1293-1308, Feb. 2016, doi: 10.1109/TWC.2015.2488634.
6. Adnan, Noor Hidayah Muhamad et al. "Massive MIMO for Fifth Generation (5G): Opportunities and Challenges." *2016 International Conference on Computer and Communication Engineering (ICCCE)* (2016): 47-52.
7. Rudolf F. Graf,P,Editor(s): Rudolf F. Graf, Modern Dictionary of Electronics (Seventh Edition),Newnes, 1999,Pages 534-604,ISBN 9780080511986, https://doi.org/10.1016/B978-0-08-051198-6.50021-7.
8. B. Mayer and R. Knochel, "Branchline-couplers with improved design flexibility and broad bandwidth," IEEE International Digest on Microwave Symposium, Dallas, TX, USA, 1990, pp. 391-394 vol.1, doi: 10.1109/MWSYM.1990.99602.
9. L. Sane, I. Dioum, K. Tall, M. M. Khouma, K. Diallo and S. M. Farssi, "Full Duplex and Pattern Reconfigurable System Antenna Design for 5G Wireless Communications Systems Using a Quadrature 3 dB Coupler," 2018 International Conference on Wireless Communications, Signal Processing and Networking (WiSPNET), Chennai, India, 2018, pp. 1-3, doi: 10.1109/WiSPNET.2018.8538709.
10. J. Reed and G. J. Wheeler, "A Method of Analysis of Symmetrical Four-Port Networks," in IRE Transactions on Microwave Theory and Techniques, vol. 4, no. 4, pp. 246-252, October 1956, doi: 10.1109/TMTT.1956.1125071.
11. Kae-Oh Sun, Sung-Jin Ho, Chih-Chuan Yen and D. van der Weide, "A compact branch-line coupler using discontinuous microstrip lines," in IEEE Microwave and Wireless Components Letters, vol. 15, no. 8, pp. 519-520, Aug. 2005, doi: 10.1109/LMWC.2005.852789.
12. Sardi, A. & ZBITOU, JAMAL & Ahmed, Errkik & El Abdellaoui, Larbi & Tajmouati, Abdelali & Latrach, Mohamed. (2014). A novel design of a microstrip 3dB coupler. International Journal of Microwave and Optical Technology. 9. 394-399.
13. N. Gupta, R. Tomar and P. Bhartia, "A Low-Loss Voltage-Controlled Analog Phase-Shifter Using Branchline Coupler and Varactor Diodes," 2007 International Conference on Microwave and Millimeter Wave Technology, Guilin, China, 2007, pp. 1-2, doi: 10.1109/ICMMT.2007.381435.

14. N. O. Parchin, R. A. Abd-Alhameed and M. Shen, "Design of Low Cost FR4 Wide-Band Antenna Arrays for Future 5G Mobile Communications," 2019 International Symposium on Antennas and Propagation (ISAP), Xi'an, China, 2019, pp. 1-3.
15. Mohd Shukor, N.A., Seman, N. 5G planar branch line coupler design based on the analysis of dielectric constant, loss tangent and quality factor at high frequency. *Sci Rep* **10**, 16115 (2020). https://doi.org/10.1038/s41598-020-72444-2
16. Zaidel, Dyg & Seman, Norhudah & Mohd Sharip, Mohd Ridhuan & Mat, Dyg & Binti Hj Mohtadzar, Nur Alia Athirah. (2017). 5G Coupler Design for Intelligent Transportation System (ITS) Application. International Journal of Electrical and Computer Engineering. 7. 899-904. 10.11591/ijece.v7i2.pp899-904.
17. Artem R. Vilenskiy, Mikhail N. Makurin, Ekaterina I. Poshisholina, and Chongmin Lee, "Design Technique for Varactor Analog Phase Shifters with Equalized Losses," Progress In Electromagnetics Research C, Vol. 86, 1-16, 2018.
18. M. L. Carneiro, M. Le Roy, A. Pérennec, R. Lababidi, P. Ferrari and V. Puyal, "Compact Analog All-Pass Phase-Shifter in 65-nm CMOS for 24/28 GHz on-Chip- and in-Package Phased-Array Antenna," 2019 IEEE 23rd Workshop on Signal and Power Integrity (SPI), 2019, pp. 1-4, doi: 10.1109/SaPIW.2019.8781643.
19. N. Singhal and S. M. R. Hasan, "A 25–30-GHz RMS Error-Minimized 360° Continuous Analog Phase Shifter Using Closed-Loop Self-Tuning I/Q Generator," in IEEE Transactions on Very Large Scale Integration (VLSI) Systems, vol. 30, no. 6, pp. 720-731, June 2022, doi: 10.1109/TVLSI.2022.3162893.
20. A. Singh and M. K. Mandal, "Electronically Tunable Reflection Type Phase Shifters," in IEEE Transactions on Circuits and Systems II: Express Briefs, vol. 67, no. 3, pp. 425-429, March 2020, doi: 10.1109/TCSII.2019.2921036.
21. T. Singh, N. K. Khaira and R. R. Mansour, "Thermally Actuated SOI RF MEMS-Based Fully Integrated Passive Reflective-Type Analog Phase Shifter for mmWave Applications," in IEEE Transactions on Microwave Theory and Techniques, vol. 69, no. 1, pp. 119-131, Jan. 2021, doi: 10.1109/TMTT.2020.3018141.
22. W. J. Liu, S. Y. Zheng, Y. M. Pan, Y. X. Li and Y. L. Long, "A wideband tunable reflection-type phase shifter with wide relative phase shift", IEEE Trans. Circuits Syst. II Exp. Briefs, vol. 64, no. 12, pp. 1442-1446, Dec. 2017.
23. T.-W. Li and H. Wang, "A millimeter-wave fully integrated passive reflection-type phase shifter with transformer-based multi-resonance loads for 360° phase shifting", IEEE Trans. Circuits Syst. I Reg. Papers, vol. 65, no. 4, pp. 1406-1419, Apr. 2018.
24. B. An, G. Chaudhary and Y. Jeong, "Wideband tunable phase shifter with low in-band phase deviation using coupled line", IEEE Microw. Wireless Compon. Lett., vol. 28, no. 8, pp. 678-680, Aug. 2018.
25. Ismail, Muhammad Faizal & Rahim, MKA & Majid, H.. (2011). The Investigation of PIN Diode Switch on Reconfigurable Antenna. 2011 IEEE International RF and Microwave Conference, RFM 2011 - Proceedings. 10.1109/RFM.2011.6168737.
26. Salem Hesari, S.; Bornemann, J. Design of a SIW Variable Phase Shifter for Beam Steering Antenna Systems. *Electronics* **2019**, *8*, 1013. https://doi.org/10.3390/electronics8091013

27. Y. Ding and K. Wu, "Varactor-tuned substrate integrated waveguide phase shifter," *2011 IEEE MTT-S International Microwave Symposium*, Baltimore, MD, USA, 2011, pp. 1-4, doi: 10.1109/MWSYM.2011.5972725.
28. Yin, Youjin et al. "Design of a cascaded full 360 ° reflection-type phase shifter with 90° hybrid coupler." *2018 IEEE MTT-S International Wireless Symposium (IWS)* (2018): 1-3.
29. Kim, S.; Jeong, J.; Chaudhary, G.; Jeong, Y. A Reflection-Type Dual-Band Phase Shifter with an Independently Tunable Phase. *Appl. Sci.* **2022**, *12*, 492. https://doi.org/10.3390/app12010492
30. ElKhorassani, M.T.; Palomares-Caballero, A.; Alex-Amor, A.; Segura-Gómez, C.; Escobedo, P.; Valenzuela-Valdés, J.F.; Padilla, P. Electronically Controllable Phase Shifter with Progressive Impedance Transformation at K Band. *Appl. Sci.* **2019**, *9*, 5229. https://doi.org/10.3390/app9235229
31. P. Padilla, A. Muñoz-Acevedo, M. Sierra-Castañer and M. Sierra-Pérez, "Electronically Reconfigurable Transmitarray at Ku Band for Microwave Applications," in IEEE Transactions on Antennas and Propagation, vol. 58, no. 8, pp. 2571-2579, Aug. 2010, doi: 10.1109/TAP.2010.2050426.
32. F. Burdin, Z. Iskandar, F. Podevin and P. Ferrari, "Design of Compact Reflection-Type Phase Shifters With High Figure-of-Merit," in *IEEE Transactions on Microwave Theory and Techniques*, vol. 63, no. 6, pp. 1883-1893, June 2015, doi: 10.1109/TMTT.2015.2428242.
33. M. Urbanski, B. Kola, K. Czuba, H. Pryschelski and F. Ludwig, "Voltage Driven Phase Shifters for Phase Reference Distribution System in SINBAD," *2020 23rd International Microwave and Radar Conference (MIKON)*, Warsaw, Poland, 2020, pp. 440-443, doi: 10.23919/MIKON48703.2020.9253786.
34. Al Ahmad, M., Kabeer, S., Sanad, A.A. and Olule, L.J.A. (2021), Compact single-varactor diode frequency-reconfigurable microstrip patch antenna. IET Microw. Antennas Propag, 15: 1100-1107. https://doi.org/10.1049/mia2.12117
35. A. Grigoriev and B. Djalilov, "Tunable antenna for mobile applications," *2016 IEEE NW Russia Young Researchers in Electrical and Electronic Engineering Conference (EIConRusNW)*, St. Petersburg, Russia, 2016, pp. 408-410, doi: 10.1109/EIConRusNW.2016.7448207.
36. Oumar, Khalid & Lai, Nai Shyan. (2019). A compact reconfigurable slotted microstrip patch antenna using pin diode for wireless applications. Journal of Physics: Conference Series. 1228. 012074. 10.1088/1742-6596/1228/1/012074.
37. F. Akbar and A. Mortazawi, "An Integrated Compact Phase Shifter With a Single Analog Control," in *IEEE Microwave and Wireless Components Letters*, vol. 32, no. 5, pp. 410-413, May 2022, doi: 10.1109/LMWC.2021.3119388.
38. A. Ray, M. K. Mandal and A. Sengupta, "Electronically Tunable Reflection Type Phase Shifter Using PIN Diode As A Variable Resistor," *2022 IEEE Microwaves, Antennas, and Propagation Conference (MAPCON)*, Bangalore, India, 2022, pp. 816-819, doi: 10.1109/MAPCON56011.2022.10047291.
39. D. D. Yang *et al.*, "Frequency Reconfigurable Hexagonal Microstrip Antenna for 5G Applications," *2021 International Conference on Microwave and Millimeter Wave Technology (ICMMT)*, Nanjing, China, 2021, pp. 1-3, doi: 10.1109/ICMMT52847.2021.9618069.
40. M. M. Amir Faisal, M. Nabil and M. Kamruzzaman, "Design and Simulation of a Single Element High Gain Microstrip Patch Antenna for 5G Wireless Communication," *2018 International*

Conference on Innovations in Science, Engineering and Technology (ICISET), 2018, pp. 290-293, doi: 10.1109/ICISET.2018.8745567.

41. Y. Rahayu, M. S. F. Reyhan, Y. B. Pradana and A. Kurniawan, "Frequency Reconfigurable 5G Rectangular Patch Antenna," *2021 26th IEEE Asia-Pacific Conference on Communications (APCC)*, Kuala Lumpur, Malaysia, 2021, pp. 19-22, doi: 10.1109/APCC49754.2021.9609869.
42. Gong, Tierui & Gavriilidis, Panagiotis & Ji, Ran & Chongwen, Huang & Alexandropoulos, George & Wei, Li & Zhang, Zhaoyang & Debbah, mérouane & Poor, H. Vincent & Yuen, Chau. (2023). Holographic MIMO Communications: Theoretical Foundations, Enabling Technologies, and Future Directions. 10.36227/techrxiv.21669656.v2.

List of information sources

1. https://www.nokia.com/networks/insights/spectrum-bands-5g-world/
2. https://halberdbastion.com/technology/cellular/5g-nr/5g-frequency-bands/n78-3500-mhz
3. https://www.avnet.com/wps/portal/abacus/solutions/markets/communications/5g-solutions/5g-beamforming/
4. https://www.youtube.com/watch?v=hhdSg9Hu0HU&t=1451s
5. https://www.youtube.com/watch?v=l4OwU1p8_tE
6. https://www.tutorialspoint.com/microwave_engineering/microwave_engineering_types_of_transmission_lines.htm
7. https://www.microwaves101.com/encyclopedias/phase-shifters
8. https://se.mathworks.com/discovery/s-parameter.html
9. https://www.antenna-theory.com/definitions/sparameters.php
10. https://www.electronicshub.org/varactor-diode/#:~:text=Equivalent%20Circuit,-For%20designing%20circuits&text=RR%20is%20the%20reverse,varactor%20diode%20should%20be%20operated.
11. https://www.infineon.com/dgdl/Infineon-BB640SERIES-DS-v01_01-en.pdf?fileId=db3a304313d846880113d9d5b10c0172
12. https://www.hioki.com/euro-en/learning/applications/detail/id_n1265218
13. http://www.ittc.ku.edu/~jstiles/723/handouts/The%20Quadrature%20Hybrid%20Coupler%20723.pdf
14. https://rfmwc.com/product-details/rf-phase-shifters
15. https://en.wikipedia.org/wiki/Starlink
16. https://www.youtube.com/watch?v=h6MfM8EFkGg
17. https://www.skyworksinc.com/-/media/SkyWorks/Documents/Products/201-300/SMV2019_to_SMV2023_Series_200074S.pdf
18. https://rfmwc.com/product-details/rf-phase-shifters#:~:text=Input%20VSWR%20of%20Phase%20shifter,the%20performance%20of%20the%20system.
19. https://www.microwaves101.com/encyclopedias/two-section-branchline-coupler
20. https://www.qorvo.com/design-hub/blog/getting-to-5g-comparing-4g-and-5g-system-requirements
21. https://www.signalboosters.com/blog/fdd-vs-tdd-explained-/#:~:text=TDD%20vs%20FDD%20Explained,and%20needs%20fewer%20base%20stations.
22. https://www.utmel.com/productdetail/skyworkssolutionsinc-smv2019079lf-7917421?gclid=CjwKCAjwg-GjBhBnEiwAMUvNWwvBsaqlRxHTjx1V0lMVOWXOj8a7s4RkyB7Vbhqkn2M7Ib3jsOLg3RoCn-8QAvD_BwE

Appendices

Appendix 1. Dimensions of the Models

Phase Shifter with a Single Section BLC

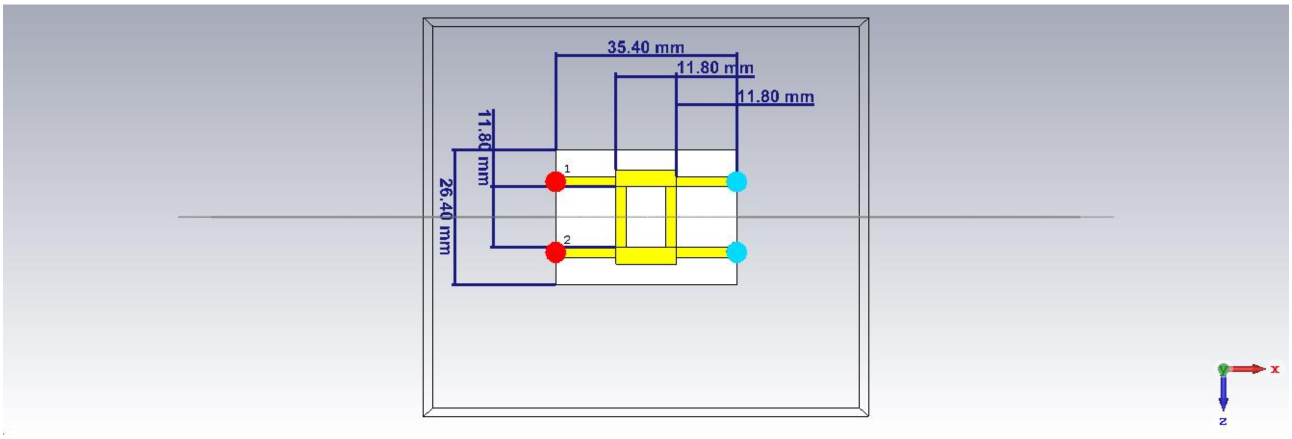

Phase Shifter with Two Sections BLC

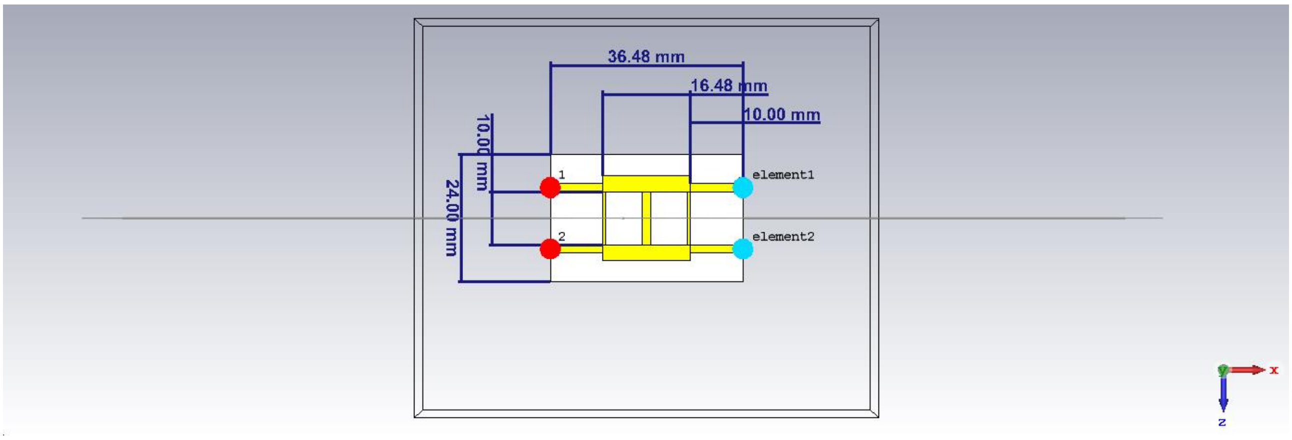

Phase Shifter with a high impedance line before the load

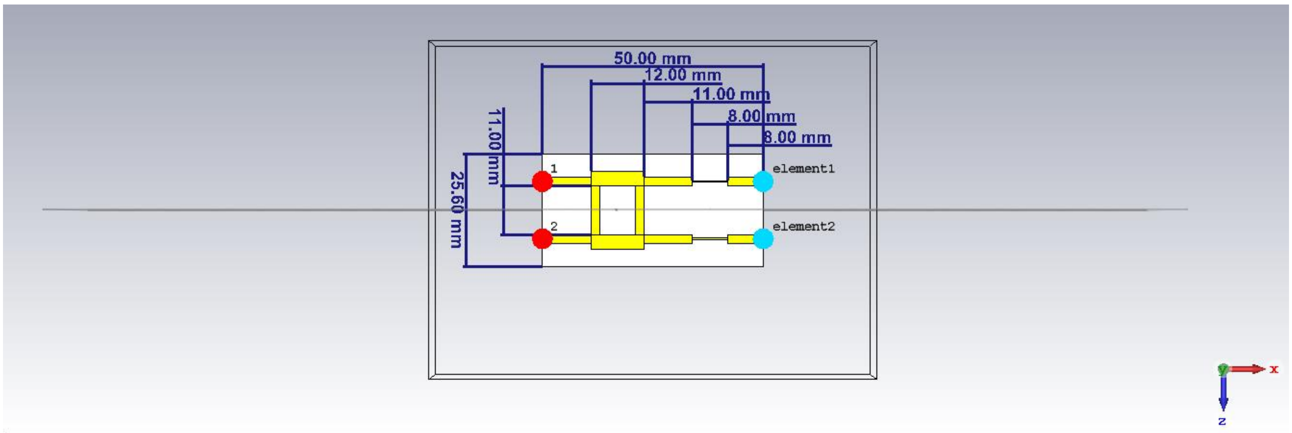

Appendix 2. Phase and S parameters

Phase Shifter with a Single Section BLC

Phase			
Capacitance (pF)	3300	3500	3800
1	10.080037	-36.508682	240.68765
2	-21.310743	-74.436037	198.59393
3	-35.183003	-90.363355	183.61812
4	-42.704828	-98.875744	176.34713
5	-47.541858	-103.99593	171.91466
6	-50.806131	-107.47315	169.02452
7	-53.174649	-109.96893	166.97661
8	-54.970183	-111.84582	165.45037
9	-56.37759	-113.30793	164.2693
10	-57.510123	-114.47872	163.32834

S11			
Capacitance (pF)	3300	3500	3800
1	-25.565581	-17.361635	-23.401791
2	-28.91316	-19.478828	-17.9152
3	-28.129797	-20.438856	-15.624819
4	-26.865149	-20.752328	-15.131784
5	-25.408297	-21.100093	-14.589017
6	-24.589956	-21.275579	-14.419324
7	-24.00538	-21.400302	-14.318811
8	-23.570463	-21.49382	-14.254577
9	-23.235522	-21.566667	-14.21114
10	-22.970172	-21.625068	-14.18046

S21			
Capacitance (pF)	3300	3500	3800
1	-1.190002	-1.4580479	-1.9709
2	-1.3948763	-1.6843809	-1.96562
3	-1.4935339	-1.7643951	-1.94687
4	-1.5431601	-1.7845719	-1.96819
5	-1.5776069	-1.8171393	-1.9167
6	-1.5994944	-1.8302742	-1.90047
7	-1.6152291	-1.8391371	-1.88777
8	-1.6270633	-1.8454799	-1.87766
9	-1.6362783	-1.8502247	-1.86945
10	-1.6436531	-1.8539004	-1.86267

Phase Shifter with Two Sections BLC

Phase of S21			
Capacitance (pF)	3300	3500	3800
1	21.075796	-31.06289	-107.90724
2	-7.8649708	-64.300773	-141.0571
3	-20.084725	-77.504423	-153.60949
4	-26.709914	-84.311015	-160.20099
5	-30.653295	-88.572664	-163.4361
6	-33.51611	-91.323161	-166.33912
7	-35.524678	-93.32584	-168.14745
8	-37.044198	-94.830838	-169.50178
9	-38.233512	-96.002762	-170.55374
10	-39.189517	-96.94097	-171.39427

S11			
Capacitance (pF)	3300	3500	3800
1	-11.971688	-18.145118	-11.450438
2	-15.457919	-15.432197	-18.317137
3	-17.808329	-15.034014	-22.784889
4	-19.420142	-15.035769	-24.812106
5	-20.257149	-15.026246	-26.036867
6	-21.14704	-15.10598	-25.561387
7	-21.697652	-15.158685	-25.29845
8	-22.115738	-15.205353	-24.998069
9	-22.441005	-15.245973	-24.718581
10	-22.69941	-15.281234	-24.473448

S21			
Capacitance (pF)	3300	3500	3800
1	-1.7269529	-1.6110785	-2.0384248
2	-1.8373744	-1.7413233	-1.7704937
3	-1.8487956	-1.8077387	-1.6258501
4	-1.8510728	-1.8446685	-1.5838433
5	-1.875013	-1.8195838	-1.579789
6	-1.8671777	-1.8504846	-1.5490334
7	-1.8700929	-1.8546775	-1.5434523
8	-1.8721781	-1.8576657	-1.5397952
9	-1.8737372	-1.8598971	-1.5372666
10	-1.8749435	-1.8616232	-1.5354434

Phase Shifter with High Impedance line before the load

Phase of S21			
Capacitance (pF)	3300 MHz	3500 MHz	3800 MHz
1	191.78879	137.9099	70.731434
2	168.9289	118.81184	54.433266
3	158.21483	109.9386	46.057925
4	152.23761	104.80908	41.618247
5	148.5139	101.65585	38.403904
6	145.96432	99.501749	36.050383
7	144.08321	97.909194	34.296857
8	142.64658	96.690771	32.937182
9	141.51321	95.727687	31.854435
10	140.59608	94.946969	30.972988

S11			
Capacitance (pF)	3300 MHz	3500 MHz	3800 MHz
1	-8.3427683	-15.529174	-17.730658
2	-10.399649	-19.016206	-16.424833
3	-11.806932	-21.087984	-15.63729
4	-12.865706	-22.348786	-15.645642
5	-13.693078	-23.477963	-15.47386
6	-14.34407	-24.406856	-15.307063
7	-14.84634	-25.122456	-15.171223
8	-15.251955	-25.705144	-15.065297
9	-15.585789	-26.186789	-14.981972
10	-15.865088	-26.186789	-14.915551

S21			
Capacitance (pF)	3300	3500	3800
1	-2.6751032	-1.62887	-1.3754998
2	-2.1669976	-1.4461174	-1.4147728
3	-1.9179496	-1.3515273	-1.5133274
4	-1.8207204	-1.3458573	-1.5454894
5	-1.7539613	-1.3426214	-1.550962
6	-1.7083513	-1.3414972	-1.5526889
7	-1.6723131	-1.3355527	-1.5697
8	-1.6448728	-1.3305666	-1.5849892
9	-1.6233876	-1.3264221	-1.5984094
10	-1.6061778	-1.3229783	-1.6100979

Phase Shifter with a Single Section BLC – PIN Diode realisation

Phase of S21			
Resistance (Ohms)	3300 MHz	3500 MHz	3800 MHz
10	-66.668062	-125.68339	152.7107
20	-63.277162	-126.56314	148.0341
30	-55.947059	-128.77147	139.11597
40	-38.440401	-138.63505	122.74912
50	10.831406	103.35077	96.037028
60	58.000924	70.501508	66.770887
70	75.062363	66.261209	46.67933
80	82.628231	64.699498	34.92545
90	86.321925	63.301001	28.048235
100	88.555152	62.630916	23.753213

S11			
Resistance (Ohms)	3300 MHz	3500 MHz	3800 MHz
10	-21.673401	-24.321983	-16.272544
20	-22.321503	-26.114511	-17.016183
30	-23.019826	-27.43985	-17.241098
40	-23.4552	-28.543207	-16.983973
50	-24.025092	-28.754171	-16.670655
60	-24.529163	-28.520572	-16.284169
70	-25.075704	-27.799997	-15.906066
80	-25.476291	-27.064122	-15.536393
90	-25.729494	-26.504473	-15.17973
100	-26.224905	-25.848428	-14.900737

S21			
Resistance (Ohms)	3300	3500	3800
10	-5.0617262	-5.4292412	-4.8352958
20	-8.6868246	-9.413657	-7.9414509
30	-12.938546	-14.410869	-11.202295
40	-18.233035	-22.427072	-14.532151
50	-22.578233	-30.537414	-16.871261
60	-19.677987	-20.061346	-16.844185
70	-16.232179	-15.81566	-15.283716
80	-13.832722	-13.296488	-13.612393
90	-12.037926	-11.597304	-12.300523
100	-10.74031	-10.36457	-11.19449

Appendix 3. VSWR of the three models at the Operating frequency

VSWR1 at 3500 MHz			
Capacitance (pF)	Model 1	Model 2	Model 3
1	1.3134584	1.2826013	1.0866199
2	1.2375967	1.4073067	1.0911252
3	1.210123	1.4305263	1.0909988
4	1.201923	1.4304205	1.0961501
5	1.1932324	1.4309945	1.1019383
6	1.1890024	1.4262168	1.10546
7	1.1860572	1.423093	1.1080031
8	1.1838815	1.4203494	1.1098715
9	1.1822059	1.417983	1.1109005
10	1.1808745	1.4159328	1.1114321